

# Viable $f(T)$ models are practically indistinguishable from $\Lambda$ CDM

S. Nesseris,<sup>1,\*</sup> S. Basilakos,<sup>2,†</sup> E. N. Saridakis,<sup>3,4,‡</sup> and L. Perivolaropoulos<sup>5,§</sup>

<sup>1</sup>*Instituto de Física Teórica UAM-CSIC, Universidad Autónoma de Madrid, Cantoblanco, 28049 Madrid, Spain*

<sup>2</sup>*Academy of Athens, Research Center for Astronomy and Applied Mathematics, Soranou Efessiou 4, 11527, Athens, Greece*

<sup>3</sup>*Physics Division, National Technical University of Athens, 15780 Zografou Campus, Athens, Greece*

<sup>4</sup>*Instituto de Física, Pontificia Universidad de Católica de Valparaíso, Casilla 4950, Valparaíso, Chile*

<sup>5</sup>*Department of Physics, University of Ioannina, 45110 Ioannina, Greece*

We investigate the cosmological predictions of several  $f(T)$  models, with up to two parameters, at both the background and the perturbation levels. Using current cosmological observations (geometric supernovae type Ia, cosmic microwave background and baryonic acoustic oscillation and dynamical growth data) we impose constraints on the distortion parameter, which quantifies the deviation of these models from the concordance  $\Lambda$  cosmology at the background level. In addition we constrain the growth index  $\gamma$  predicted in the context of these models using the latest perturbation growth data in the context of three parametrizations for  $\gamma$ . The evolution of the best fit effective Newton constant, which incorporates the  $f(T)$ -gravity effects, is also obtained along with the corresponding  $1\sigma$  error regions. We show that all the viable parameter sectors of the  $f(T)$  gravity models considered practically reduce these models to  $\Lambda$ CDM. Thus, the degrees of freedom that open up to  $\Lambda$ CDM in the context of  $f(T)$  gravity models are not utilized by the cosmological data leading to an overall disfavor of these models.

PACS numbers: 95.36.+x, 98.80.-k, 04.50.Kd, 98.80.Es

## I. INTRODUCTION

The  $\Lambda$ CDM model is currently the simplest model consistent with practically all cosmological observations. It assumes homogeneity and isotropy on large cosmological scales and the presence of a cosmological constant  $\Lambda$  in the context of general relativity. Despite of its simplicity and its overall consistency with observations,  $\Lambda$ CDM has two weak points:

1. It requires a theoretically unnatural and fine-tuned value for  $\Lambda$ .
2. It is marginally consistent with some recent large scale cosmological observations (for instance the cosmic microwave background anomalies).

Motivated by these two weak points, a wide range of more complex generalized cosmological models has been investigated. Most of these models reduce to  $\Lambda$ CDM for specific values of their parameters. They can be classified in two broad classes: Modified gravity models constitute the one class (see for instance [1]), with the other being the scalar field dark energy that adheres to general relativity (see for instance [2, 3]). Among the variety of modified gravity theories,  $f(T)$  gravity has recently gained a lot of attention. It is based on the old formulation of the teleparallel equivalent of general relativity (TEGR) [4–6]. In teleparallel formulations the dynamical fields are the four linearly independent vierbeins, while

one uses the curvatureless Weitzenböck connection instead of the torsionless Levi-Civita one. Thus, one can construct the torsion tensor, which includes all the information concerning the gravitational field, and then by suitable contractions one can write down the corresponding Lagrangian density  $T$  [5] (assuming invariance under general coordinate transformations, global Lorentz and parity transformations, and requiring up to second-order terms of the torsion tensor). Finally,  $f(T)$  gravity arises as a natural extension of TEGR, if one generalizes the Lagrangian to be a function of  $T$  [7–9], inspired by the well-known extension of  $f(R)$  Einstein-Hilbert action. However, the significant advantage is that although the curvature tensor contains second-order derivatives of the metric and thus  $f(R)$  gravity gives rise to fourth-order equations which may lead to pathologies, the torsion tensor includes only products of first derivatives of the vierbeins, giving rise to second-order field equations.

Although TEGR coincides completely with general relativity both at the background and perturbation levels,  $f(T)$  gravity exhibits novel structural and phenomenological features. In particular, imposing a cosmological background one can extract various cosmological solutions, consistent with the observable behavior [7–13]. Additionally, imposing spherical geometry one can investigate the spherical, black-hole solutions of  $f(T)$  gravity [14]. However, we stress that although TEGR coincides with GR,  $f(T)$  gravity does not coincide with  $f(R)$  extension, but it rather constitutes a different class of modified gravity.

One crucial question is what classes of  $f(T)$  extensions are allowed by observations. At the theoretical level, the aforementioned cosmological and spherical solutions lead to a variety of such expressions. However, taking into account observational data, either from cosmological [11,

\*Electronic address: savvas.nesseris@uam.es

†Electronic address: svasil@academyofathens.gr

‡Electronic address: Emmanuel.Saridakis@baylor.edu

§Electronic address: leandros@uoi.gr

12, 15, 16] as well as from Solar System observations [13], one can show that the deviations from TEGR must be small.

In the present work we are interested in constraining the  $f(T)$  forms using the latest cosmological data, both at the background and perturbation levels. In order to do so we need to define the Hubble parameter as a function of redshift. The issue of using iterative techniques in order to treat the Hubble expansion in  $f(R)$  gravity has been proposed by Starobinsky in Ref. [17]. Furthermore, in a recent paper some of us [18] used a new iterative approach in order to observationally constrain deviations of  $f(R)$  models from  $\Lambda$ CDM and general relativity. In this context, we first showed that all known viable  $f(R)$  models may be written as perturbations around  $\Lambda$ CDM with a deviation parameter we called  $b$  (for  $b = 0$  these models reduce to  $\Lambda$ CDM). Using a novel perturbative iterative technique we were able to construct analytic cosmological expansion solutions of a highly nonlinear and stiff system of ordinary differential equations and impose cosmological observational constraints on the deviation parameter  $b$ .

We also showed that the observationally viable  $f(R)$  models effectively include the cosmological constant even though they were proposed as being free from a cosmological constant in the original  $f(R)$  papers [17, 19]. Inspired by our previous similar work on  $f(R)$  gravity [18], we extend it to the case of  $f(T)$  gravity models and use the standard joint likelihood analysis of the recent supernovae type Ia data (SnIa), the cosmic microwave background (CMB) shift parameters, the baryonic acoustic oscillations (BAO) and the growth rate data provided by the various galaxy surveys. Based on these cosmological observations we identify the viable range of parameters of five previously proposed  $f(T)$  models. Additionally, comparing the resulting analytical expressions of the  $f(T)$  Hubble parameter with the numerical solutions at low and intermediate redshifts, we verify that our iterative perturbative technique is highly accurate.

The plan of the work is as follows: In Sec. II we briefly discuss the main properties of the  $f(T)$  gravity, while in Sec. III we apply the  $f(T)$  gravity in a cosmological framework, providing the relevant equations both at the background and perturbation levels. In Sec. IV we present and we analytically elaborate on all the  $f(T)$  models of the literature with two parameters (out of which one is independent). In Sec. V we impose observational constraints, utilizing three parametrizations of the growth index. Finally, the main conclusions are summarized in Sec. VI.

## II. $f(T)$ GRAVITY

In this section we briefly review the  $f(T)$  gravitational paradigm. In this construction the dynamical variables

are the vierbein fields  $\mathbf{e}_A(x^\mu)$ <sup>1</sup>. The vierbeins at each point  $x^\mu$  of the manifold form an orthonormal basis for the tangent space, that is  $\mathbf{e}_A \cdot \mathbf{e}_B = \eta_{AB}$ , with  $\eta_{AB} = \text{diag}(1, -1, -1, -1)$ , and they can be expressed in terms of the components  $e_A^\mu$  in a coordinate basis as  $\mathbf{e}_A = e_A^\mu \partial_\mu$ . Therefore, the metric tensor is obtained from the dual vierbein through

$$g_{\mu\nu}(x) = \eta_{AB} e_A^\mu(x) e_B^\nu(x). \quad (1)$$

While in usual gravitational formalism one uses the torsionless Levi-Civita connection, in the present formulation one uses the curvatureless Weitzenböck connection defined as  $\overset{\mathbf{w}}{\Gamma}_{\nu\mu}^\lambda \equiv e_A^\lambda \partial_\mu e_\nu^A$  [20], and the corresponding torsion tensor is written as

$$T_{\mu\nu}^\lambda = \overset{\mathbf{w}}{\Gamma}_{\nu\mu}^\lambda - \overset{\mathbf{w}}{\Gamma}_{\mu\nu}^\lambda = e_A^\lambda (\partial_\mu e_\nu^A - \partial_\nu e_\mu^A). \quad (2)$$

Furthermore, the contorsion tensor, which provides the difference between Weitzenböck and Levi-Civita connections, is given by  $K^{\mu\nu}{}_\rho \equiv -\frac{1}{2} (T^{\mu\nu}{}_\rho - T^{\nu\mu}{}_\rho - T_\rho{}^{\mu\nu})$ , while for convenience we define  $S_\rho{}^{\mu\nu} \equiv \frac{1}{2} (K^{\mu\nu}{}_\rho + \delta_\rho^\mu T^{\alpha\nu}{}_\alpha - \delta_\rho^\nu T^{\alpha\mu}{}_\alpha)$ . Finally, imposing coordinate, Lorentz and parity symmetries, and the additional requirement the Lagrangian to be second order in the torsion tensor [5, 6], one obtains the teleparallel Lagrangian (called ‘‘torsion scalar’’ too)

$$T \equiv \frac{1}{4} T^{\rho\mu\nu} T_{\rho\mu\nu} + \frac{1}{2} T^{\rho\mu\nu} T_{\nu\mu\rho} - T_{\rho\mu}{}^\rho T^{\nu\mu}{}_\nu. \quad (3)$$

Thus, in the teleparallel gravitational paradigm, all the information concerning the gravitational field is embedded in the torsion tensor  $T_{\mu\nu}^\lambda$ , which produces the torsion scalar  $T$  in a similar way as the curvature Riemann tensor gives rise to the Ricci scalar in standard general relativity.

In the teleparallel equivalent of general relativity the action is just  $T$ . However, one can be inspired by the  $f(R)$  extensions of general relativity and extend  $T$  to a function  $T + f(T)$ . Therefore, the corresponding action of  $f(T)$  gravity reads as

$$I = \frac{1}{16\pi G_N} \int d^4x e [T + f(T)], \quad (4)$$

where  $e = \det(e_A^\mu) = \sqrt{-g}$ ,  $G_N$  is the gravitational constant, and we use units where the light speed is equal to 1. Lastly, TEGR and thus general relativity is restored when  $f(T) = 0$ , while if  $f(T) = \text{const}$  we recover general relativity with a cosmological constant.

<sup>1</sup> Throughout the manuscript, greek indices  $\mu, \nu, \dots$  and capital Latin indices  $A, B, \dots$  run over all coordinate and tangent spacetime 0, 1, 2, 3, while lower case latin indices (from the beginning of the alphabet)  $a, b, \dots$  and lower case latin indices (from the middle of the alphabet)  $i, j, \dots$ , run over tangent-space and spatial coordinates 1, 2, 3 respectively.

### III. $f(T)$ COSMOLOGY

We now proceed to the cosmological application of  $f(T)$  gravity. In order to construct a realistic cosmology we have to incorporate in the action the matter and the radiation sectors respectively. Therefore, the total action is written as

$$I = \frac{1}{16\pi G_N} \int d^4x e [T + f(T) + L_m + L_r], \quad (5)$$

where the matter and radiation Lagrangians are assumed to correspond to perfect fluids with energy densities  $\rho_m$ ,  $\rho_r$  and pressures  $P_m$ ,  $P_r$  respectively.

Secondly, in order to examine a universe governed by  $f(T)$  gravity, we have to impose the usual homogeneous and isotropic geometry. Therefore, we consider the common choice for the vierbein form, that is,

$$e_\mu^A = \text{diag}(1, a, a, a), \quad (6)$$

which corresponds to a flat Friedmann-Robertson-Walker (FRW) background geometry with metric

$$ds^2 = dt^2 - a^2(t) \delta_{ij} dx^i dx^j, \quad (7)$$

with  $a(t)$  the scale factor.

#### A. Background behavior

Varying the action (5) with respect to the vierbeins we acquire the field equations

$$\begin{aligned} e^{-1} \partial_\mu (e e_A^\rho S_\rho^{\mu\nu}) [1 + f_T] + e_A^\rho S_\rho^{\mu\nu} \partial_\mu (T) f_{TT} \\ - [1 + f_T] e_A^\lambda T^\rho_{\mu\lambda} S_\rho^{\nu\mu} + \frac{1}{4} e_A^\nu [T + f(T)] \\ = 4\pi G e_A^\rho T^{\text{em}}{}_\rho{}^\nu, \end{aligned} \quad (8)$$

where  $f_T = \partial f / \partial T$ ,  $f_{TT} = \partial^2 f / \partial T^2$ , and  $T^{\text{em}}{}_\rho{}^\nu$  stands for the usual energy-momentum tensor.

Inserting the vierbein choice (6) into the field equations (8) we obtain the modified Friedmann equations

$$H^2 = \frac{8\pi G_N}{3} (\rho_m + \rho_r) - \frac{f}{6} + \frac{T f_T}{3} \quad (9)$$

$$\dot{H} = -\frac{4\pi G_N (\rho_m + P_m + \rho_r + P_r)}{1 + f_T + 2T f_{TT}}, \quad (10)$$

where  $H \equiv \dot{a}/a$  is the Hubble parameter, with the dot denoting derivatives with respect to the cosmic time  $t$ . We mention that in order to bring the Friedmann equations closer to their standard form, we used the relation

$$T = -6H^2, \quad (11)$$

which through (3) arises straightforwardly for a FRW universe.

Observing the form of the first Friedmann equation (9), and comparing to the usual one, we deduce that in the scenario at hand we obtain an effective dark energy sector of (modified) gravitational origin. In particular, one can define the dark energy density and pressure as [9]

$$\rho_{DE} \equiv \frac{3}{8\pi G_N} \left[ -\frac{f}{6} + \frac{T f_T}{3} \right], \quad (12)$$

$$P_{DE} \equiv \frac{1}{16\pi G_N} \left[ \frac{f - f_T T + 2T^2 f_{TT}}{1 + f_T + 2T f_{TT}} \right], \quad (13)$$

while its effective equation-of-state parameter reads:

$$w = -\frac{f/T - f_T + 2T f_{TT}}{[1 + f_T + 2T f_{TT}] [f/T - 2f_T]}. \quad (14)$$

In order to quantitatively elaborate the above modified Friedmann equations, and confront them with observations, we follow the usual procedure. Firstly we define

$$E^2(z) \equiv \frac{H^2(z)}{H_0^2} = \frac{T(z)}{T_0}, \quad (15)$$

where  $T_0 \equiv -6H_0^2$ . Also, we have used the redshift  $z = \frac{a_0}{a} - 1$  as the independent variable and denoted by “0” the current value of a quantity (in the following we set  $a_0 = 1$ ). Thus, using also that  $\rho_m = \rho_{m0}(1+z)^3$ ,  $\rho_r = \rho_{r0}(1+z)^4$ , we can rewrite the first Friedmann equation (9) as

$$E^2(z, \mathbf{r}) = \Omega_{m0}(1+z)^3 + \Omega_{r0}(1+z)^4 + \Omega_{F0} y(z, \mathbf{r}) \quad (16)$$

with

$$\Omega_{F0} = 1 - \Omega_{m0} - \Omega_{r0}, \quad (17)$$

where  $\Omega_{i0} = \frac{8\pi G \rho_{i0}}{3H_0^2}$  is the corresponding density parameter at present. Therefore, the effect of the  $f(T)$  gravity is quantified by the function  $y(z, \mathbf{r})$  (normalized to unity at present time), which depends on  $\Omega_{m0}, \Omega_{r0}$ , as well as on the  $f(T)$ -form parameters  $r_1, r_2, \dots$ , and it is of the form

$$y(z, \mathbf{r}) = \frac{1}{T_0 \Omega_{F0}} [f - 2T f_T]. \quad (18)$$

According to Eq.(11) the additional term (18) in the effective Friedman equation (16) induced by the  $f(T)$  term is a function of the Hubble parameter only. Thus, this term is not completely arbitrary and cannot reproduce any arbitrary expansion history. As we will show further below, the interesting point of the current analysis is that the particular range of degrees of freedom representing deviations from  $\Lambda$ CDM in the context of  $f(T)$  models is not favored by cosmological observations.

#### B. Linear matter perturbations

We now briefly discuss the linear matter perturbations of  $f(T)$  gravity. We first review the standard treatment

of perturbations for general dark energy or modified gravity scenarios. In this analysis, the extra information is quantified by the effective Newton's gravitational constant, which appears in the various observables such as the growth index. Thus, inserting in these expressions the calculated effective Newton's gravitational constant of  $f(T)$  gravity, we obtain the corresponding perturbation observables of  $f(T)$  cosmology.

In the framework of any dark energy model, including those of modified gravity ("geometrical dark energy"), it is well known that at the subhorizon scales the dark energy component is expected to be smooth, and thus we can consider perturbations only on the matter component of the cosmic fluid [21]. We refer the reader to Refs. [18, 22–27] for full details of the calculation, summarizing only the relevant results in this section.

The basic equation which governs the behavior of the matter perturbations in the linear regime is written as

$$\ddot{\delta}_m + 2H\dot{\delta}_m = 4\pi G_{\text{eff}}\rho_m\delta_m, \quad (19)$$

where  $\rho_m$  is the matter density and  $G_{\text{eff}}(a) = G_N Q(a)$ , with  $G_N$  denoting Newton's gravitational constant. That is, the effect of the modified gravity at the linear perturbation level is reflected in an effective Newton's gravitational constant  $G_{\text{eff}}(a)$ , which in general is evolving. Finally, in the above analysis it has been found that  $\delta_m(t) \propto D(t)$ , where  $D(t)$  is the linear growth factor normalized to unity at present time.

In the case of general-relativity-based scalar-field dark energy models, we obviously have  $G_{\text{eff}}(a) = G_N$  [that is  $Q(a) = 1$ ] and therefore (19) reduces to the usual time-evolution equation for the mass density contrast [28]. Moreover, in the case of the usual  $\Lambda$  cosmology, one can solve (19) analytically in order to obtain the growth factor [28]

$$D_\Lambda(z) = \frac{5\Omega_{m0}E_\Lambda(z)}{2} \int_z^{+\infty} \frac{(1+u)du}{E_\Lambda^3(u)}, \quad (20)$$

where

$$E_\Lambda(z) = [\Omega_{m0}(1+z)^3 + 1 - \Omega_{m0}]^{1/2} \quad (21)$$

in the matter dominated era.

In general for either dark energy or modified gravity scenarios, a useful tool that simplifies the numerical calculations significantly is the growth rate of clustering [28]

$$F(a) = \frac{d \ln \delta_m}{d \ln a} \simeq \Omega_m^\gamma(a), \quad (22)$$

where  $\gamma$  is the growth index, which is general evolving. The growth index is very important since it can be used to distinguish between general relativity and modified gravity on cosmological scales. Indeed, for a constant dark energy equation of state parameter  $w$ , dark energy scenarios in the framework of general relativity the growth index is well approximated by  $\gamma \simeq \frac{3(w-1)}{6w-5}$  [23, 29–32], which reduces to  $\approx 6/11$  for the concordance  $\Lambda$  cosmology ( $w = -1$ ). On the other hand, for the braneworld

model of Dvali, Gabadadze and Porrati [33] the growth index becomes  $\gamma \approx 11/16$  [31, 34–36], for some  $f(R)$  gravity models one acquires  $\gamma \simeq 0.415 - 0.21z$  for various parameter values [22, 37], while for Finsler-Randers cosmology we have  $\gamma \approx 9/14$  [38].

Generally, combining Eq. (19) with the first equality of (22) we obtain

$$a \frac{dF(a)}{da} + F(a)^2 + X(a)F(a) = \frac{3}{2}\Omega_m(a)Q(a), \quad (23)$$

with

$$X(a) = \frac{1}{2} - \frac{3}{2}w(a)[1 - \Omega_m(a)], \quad (24)$$

where we have used that [2, 3, 18, 39]

$$w(a) = \frac{-1 - \frac{2}{3}a \frac{d \ln E}{da}}{1 - \Omega_m(a)}, \quad (25)$$

$$\Omega_m(a) = \frac{\Omega_{m0}a^{-3}}{E^2(a)}, \quad (26)$$

and

$$\frac{d\Omega_m(a)}{da} = \frac{3}{a}w(a)\Omega_m(a)[1 - \Omega_m(a)]. \quad (27)$$

Concerning the functional form of the growth index we consider various situations. The simplest one is to use a constant growth index (hereafter  $\Gamma_0$  model). If we allow  $\gamma$  to be a function of redshift then Eq.(23) can be expressed in terms of  $\gamma = \gamma(z)$  and it is given by

$$-(1+z)\gamma' \ln(\Omega_m) + \Omega_m^\gamma + 3w(1 - \Omega_m) \left( \gamma - \frac{1}{2} \right) + \frac{1}{2} = \frac{3}{2}Q\Omega_m^{1-\gamma}, \quad (28)$$

where prime denotes derivative with respect to redshift. Writing the above equation at the present epoch ( $z = 0$ ) we have

$$-\gamma'(0) \ln(\Omega_{m0}) + \Omega_{m0}^{\gamma(0)} + 3w_0(1 - \Omega_{m0}) \left[ \gamma(0) - \frac{1}{2} \right] + \frac{1}{2} = \frac{3}{2}Q_0\Omega_{m0}^{1-\gamma(0)}, \quad (29)$$

where  $Q_0 = Q(z = 0)$  and  $w_0 = w(z = 0)$ .

In this work we consider some well known  $\gamma(z)$  functional forms (see [40–43]). These parametrizations are

$$\gamma(z) = \begin{cases} \gamma_0, & \Gamma_0 \text{ model} \\ \gamma_0 + \gamma_1 z, & \Gamma_1 \text{ model} \\ \gamma_0 + \gamma_1(1-a), & \Gamma_2 \text{ model.} \end{cases} \quad (30)$$

Inserting the  $\Gamma_{1-2}$  formulas into Eq.(29) one can easily write the parameter  $\gamma_1$  in terms of  $\gamma_0$ :

$$\gamma_1 = \frac{\Omega_{m0}^{\gamma_0} + 3w_0(\gamma_0 - \frac{1}{2})(1 - \Omega_{m0}) - \frac{3}{2}Q_0\Omega_{m0}^{1-\gamma_0} + \frac{1}{2}}{\ln \Omega_{m0}}. \quad (31)$$

Finally, we would like to stress that the  $\Gamma_1$  parametrization is valid only at relatively low redshifts  $0 \leq z \leq 0.5$ . Therefore, in the statistical analysis presented below we utilize a constant growth index, namely,  $\gamma = \gamma_0 + 0.5\gamma_1$  for  $z > 0.5$ .

Since we now have the general perturbation formulation, we just need to insert  $G_{\text{eff}}(a)$ , or equivalently  $Q(a)$ , of  $f(T)$  gravity in the above relations. Unlike the  $f(R)$  gravity, the effective Newton's parameter in  $f(T)$  gravity is not affected by the scale but rather it takes the following form [44]:

$$Q(a) = \frac{G_{\text{eff}}(a)}{G_N} = \frac{1}{1 + f_T}, \quad (32)$$

as it arises from the complete perturbation analysis [47]. The above can be understood, as it was shown in Ref.[45], from the fact that the  $f(T)$  cosmological scenario can be rewritten as the K-essence model which implies that since we remain at the Jordan frame we do not expect to have a  $k$  dependence in the effective Newton's parameter and thus in the growth factor. However, doing a similar exercise for the  $f(R)$  gravity [see Eqs. (8) (10) in Ref.[46]] one can easily find that it corresponds to a scalar-tensor theory, i.e. a nonminimally coupled scalar field which obviously induces a  $k$  dependence in the matter density perturbations. Therefore, in the rest of the work we apply the above analysis in the case of  $f(T)$ , that is, with  $Q(a)$  given by (32).

#### IV. SPECIFIC $f(T)$ MODELS AND THE DEVIATION FROM $\Lambda$ CDM

In this section we review all the specific  $f(T)$  models that have appeared in the literature, with two parameters out of which one is independent. We calculate the function  $y(z, \mathbf{r})$  using (18) and their  $G_{\text{eff}}(a)$  using (32). We quantify the deviation of the function  $y(z, \mathbf{r})$  from its  $\Lambda$ CDM value (constant) through a distortion parameter  $b$ . The considered models are as follows.

1. The power-law model of Bengochea and Ferraro (hereafter  $f_1$ CDM) [8], with

$$f(T) = \alpha(-T)^b, \quad (33)$$

where  $\alpha$  and  $b$  are the two model parameters. Substituting this  $f(T)$  form into the modified Friedmann equation (9) at present, we obtain

$$\alpha = (6H_0^2)^{1-b} \frac{\Omega_{F0}}{2b-1}, \quad (34)$$

while (18) gives

$$y(z, b) = E^{2b}(z, b). \quad (35)$$

Additionally, the effective Newton's constant from (32) becomes

$$G_{\text{eff}}(z) = \frac{G_N}{1 + \frac{b\Omega_{F0}}{(1-2b)E^{2(1-b)}}}. \quad (36)$$

It is evident that for  $b$  strictly equal to zero the  $f_1$ CDM model reduces to  $\Lambda$ CDM cosmology, namely  $T + f(T) = T - 2\Lambda$  (where  $\Lambda = 3\Omega_{F0}H_0^2$ ,  $\Omega_{F0} = \Omega_{\Lambda 0}$ ), while for  $b = 1/2$  it reduces to the Dvali, Gabadadze and Porrati (DGP) ones [33]. Note that in order to obtain an accelerating expansion, it is required that  $b < 1$ .

2. The Linder model (hereafter  $f_2$ CDM) [9]

$$f(T) = \alpha T_0(1 - e^{-p\sqrt{T/T_0}}), \quad (37)$$

with  $\alpha$  and  $p$  the two model parameters. In this case from (9) we find that

$$\alpha = \frac{\Omega_{F0}}{1 - (1+p)e^{-p}}, \quad (38)$$

and from (18) we acquire

$$y(z, p) = \frac{1 - (1+pE)e^{-pE}}{1 - (1+p)e^{-p}}, \quad (39)$$

while from (32) we obtain

$$G_{\text{eff}}(z) = \frac{G_N}{1 + \frac{\Omega_{F0}p e^{-pE}}{2E[1 - (1+p)e^{-p}]}}. \quad (40)$$

Thus, for  $p \rightarrow +\infty$  the  $f_2$ CDM reduces to  $\Lambda$ CDM cosmology, since

$$\lim_{p \rightarrow +\infty} [T + f(T)] = T - 2\Lambda. \quad (41)$$

The parameter  $p$  of the present  $f_2$ CDM model has a different interpretation comparing to  $b$  for the  $f_1$ CDM model, since the two models are obviously different. However, since in the limiting case they both reduce to  $\Lambda$ CDM paradigm, we can rewrite the present  $f_2$ CDM model replacing  $p = 1/b$ . In this case (39) leads to

$$y(z, b) = \frac{1 - (1 + \frac{E}{b})e^{-E/b}}{1 - (1 + \frac{1}{b})e^{-1/b}}, \quad (42)$$

which indeed tends to unity for  $b \rightarrow 0^+$ .

3. Motivated by exponential  $f(R)$  gravity [48], one can construct the following  $f(T)$  model (hereafter  $f_3$ CDM):

$$f(T) = \alpha T_0(1 - e^{-pT/T_0}), \quad (43)$$

with  $\alpha$  and  $p$  the two model parameters. In this case we obtain

$$\alpha = \frac{\Omega_{F0}}{1 - (1+2p)e^{-p}}, \quad (44)$$

$$y(z, p) = \frac{1 - (1 + 2pE^2)e^{-pE^2}}{1 - (1 + 2p)e^{-p}}. \quad (45)$$

and

$$G_{\text{eff}}(z) = \frac{G_N}{1 + \frac{\Omega_{F0} p e^{-pE^2}}{1 - (1+2p)e^{-p}}} . \quad (46)$$

Similarly to the previous case we can rewrite  $f_3$ CDM model using  $p = 1/b$ , obtaining

$$y(z, b) = \frac{1 - (1 + \frac{2E^2}{b})e^{-E^2/b}}{1 - (1 + \frac{2}{b})e^{-1/b}} . \quad (47)$$

Again, we see that for  $p \rightarrow +\infty$ , or equivalently for  $b \rightarrow 0^+$ , the  $f_3$ CDM model tends to the  $\Lambda$ CDM cosmology.

4. The Bamba *et al.* logarithmic model (hereafter  $f_4$ CDM) [49]

$$f(T) = \alpha T_0 \sqrt{\frac{T}{qT_0}} \ln\left(\frac{qT_0}{T}\right) \quad (48)$$

with  $\alpha$  and  $q$  the two model parameters. In this case we obtain

$$\alpha = \frac{\Omega_{F0} \sqrt{q}}{2} , \quad (49)$$

$$y(z) = E(z) , \quad (50)$$

and

$$G_{\text{eff}}(z) = \frac{G_N}{1 + \frac{\Omega_{F0}}{2E} \left[ \ln\left(\frac{\sqrt{q}}{E}\right) - 1 \right]} . \quad (51)$$

The fact that the distortion function does not depend on the model parameters, allows us to write (16) as

$$E(z) = \frac{1}{2} \sqrt{\Omega_{F0}^2 + 4 [\Omega_{m0}(1+z)^3 + \Omega_{r0}(1+z)^4]} + \frac{\Omega_{F0}}{2} . \quad (52)$$

Interestingly enough, from the above relation we deduce that at the background level the  $f_4$ CDM model coincides with the flat DGP one (with  $\Omega_{F0} = \Omega_{DGP}$ ), which implies that the two nonstandard gravity models are cosmologically equivalent as far as the cosmic expansion is concerned, in spite of the fact that the two models have a completely different geometrical basis. At the perturbative level, however, we do expect to find differences between  $f_4$ CDM and DGP, since  $G_{\text{eff}}(z)$  evolves differently in two models [in flat DGP gravity we have  $\frac{G_{\text{eff}}(z)}{G_N} = \frac{2+4\Omega_m^2(z)}{3+3\Omega_m^2(z)}$ ].

Notice that this model does not give  $\Lambda$ CDM cosmology for any value of its parameters. However, in this work we are interested in the viable  $f(T)$ ,

in the sense that these  $f(T)$  models can describe the matter and dark energy eras as well as they are consistent with the observational data (including Solar System tests), and finally they have stable perturbations. Although these necessary analysis have not yet been performed for all the above  $f(T)$  models, a failure of a particular model to pass one of these is enough to exclude it. Therefore, since the present  $f_4$ CDM model coincides with DGP at the background level, it inherits its disadvantages concerning the confrontation with observations. Thus, as anticipated from previous studies [50], we verify in the following section that this model is nonviable when tested using the latest cosmological observations.

5. The hyperbolic-tangent model (hereafter  $f_5$ CDM) [51]

$$f(T) = \alpha (-T)^n \tanh\left(\frac{T_0}{T}\right) \quad (53)$$

with  $\alpha$  and  $n$  the two model parameters. In this case we obtain

$$\alpha = -\frac{\Omega_{F0}(6H_0)^{1-n}}{[2\text{sech}^2(1) + (1-2n)\tanh(1)]} , \quad (54)$$

$$y(z, n) = E^{2(n-1)} \frac{2\text{sech}^2\left(\frac{1}{E^2}\right) + (1-2n)E^2 \tanh\left(\frac{1}{E^2}\right)}{2\text{sech}^2(1) + (1-2n)\tanh(1)} \quad (55)$$

and

$$G_{\text{eff}}(z) = \frac{G_N}{1 + \frac{\Omega_{F0} E^{2(n-2)} [nE^2 \tanh\left(\frac{1}{E^2}\right) - \text{sech}^2\left(\frac{1}{E^2}\right)]}{2\text{sech}^2(1) + (1-2n)\tanh(1)}} . \quad (56)$$

The  $f_5$ CDM model does not give  $\Lambda$ CDM cosmology for any value of its parameters. However, as we show in the next section, this model is in mild tension with the data as it has a best fit  $\chi_{\text{min}}^2 = (579.583, 580.723, 578.027)$  for the  $\Gamma_0$ ,  $\Gamma_1$  and  $\Gamma_2$  growth rate parameterizations respectively, which is significantly larger than that of  $f_{1-3}$ CDM and  $\Lambda$ CDM models respectively (see Table I). Additionally the current  $f(T)$  model has one more free parameter. For the reasons developed above we consider it as nonviable (see also akaike information criterion (AIC) test in Table I.)

The above five  $f(T)$  forms are the ones that have been used in the literature of  $f(T)$  cosmology, possessing up to two parameters, out of which one is independent. Clearly, in principle one could additionally consider their combinations too; however, the appearance of many free parameters would be a significant disadvantage. Therefore, in the present work we focus only on these five elementary *Ansätze*.

As we showed, for the first three the distortion parameter measures the smooth deviation from the  $\Lambda$ CDM

model. The other two models do not have  $\Lambda$ CDM cosmology as a limiting case; however, as we show in the next section, they are in tension with observations. Thus, in the rest of this section we focus on the first three models, namely on  $f_{1-3}$ CDM ones.

Having performed the above elaboration of various  $f(T)$  models, we can now follow the procedure and iterative techniques of Basilakos, Nesseris and Perivolaropoulos [18], in which we have shown that all the observationally viable  $f(R)$  parameterizations can be expressed as perturbations deviating from  $\Lambda$ CDM cosmology.

For the  $f_1$ CDM model there are two different, but complementary, ways we can find analytical approximations for the Hubble parameter. The first method involves doing a Taylor expansion of  $E^2(z, b)$  around  $b = 0$ , while in the second we perform the Taylor expansion in the modified Friedman equation directly. Below, we briefly review and test both methods, called  $M_1$  and  $M_2$  respectively.

First, from (16) with (35) we can write explicitly the Hubble parameter for the  $f_1$ CDM model as

$$E^2(z, b) = \Omega_{m0}(1+z)^3 + \Omega_{r0}(1+z)^4 + \Omega_{F0} y(z, b), \quad (57)$$

where

$$y(z, b) = E^{2b}(z, b). \quad (58)$$

Obviously, in Eq. (57) if we set  $b$  strictly equal to zero then we get the Hubble parameter for the  $\Lambda$ CDM model

$$E^2(z, 0) = \Omega_{m0}(1+z)^3 + \Omega_{r0}(1+z)^4 + \Omega_{F0} \equiv E_\Lambda^2(z). \quad (59)$$

Now, performing a Taylor expansion, up to second order, on  $E^2(z, b)$  around  $b = 0$  and with the help of (57) we arrive at

$$\begin{aligned} E^2(z, b) &= E^2(z, 0) + \left. \frac{dE^2(z, b)}{db} \right|_{b=0} b + \left. \frac{d^2 E^2(z, b)}{db^2} \right|_{b=0} \frac{b^2}{2} + \dots = \\ &= E_\Lambda^2(z) + \Omega_{F0} \left. \frac{dy(z, b)}{db} \right|_{b=0} b + \Omega_{F0} \left. \frac{d^2 y(z, b)}{db^2} \right|_{b=0} \frac{b^2}{2} + \dots \end{aligned} \quad (60)$$

The terms involving the derivatives of  $y(z, b)$  can readily be calculated from Eq. (58) as

$$\frac{dy(z, b)}{db} = 2E(z, b)^{2b} \left\{ \frac{b}{E(z, b)} \frac{dE(z, b)}{db} + \ln [E(z, b)] \right\}, \quad (61)$$

and evaluating the above equation for  $b = 0$  we have

$$\left. \frac{dy(z, b)}{db} \right|_{b=0} = 2 \ln [E(z, 0)] = \ln [E_\Lambda^2(z)]. \quad (62)$$

Similarly for the second derivative term we have

$$\left. \frac{d^2 y(z, b)}{db^2} \right|_{b=0} = \frac{2\Omega_{F0} \ln [E_\Lambda^2(z)]}{E_\Lambda^2(z)} + \ln [E_\Lambda^2(z)]^2. \quad (63)$$

Thus, the Taylor expansion up to second order for the first method  $M_1$  becomes

$$\begin{aligned} E^2(z, b) &= E_\Lambda^2(z) + \Omega_{F0} \ln [E_\Lambda^2(z)] b \\ &+ \Omega_{F0} \left\{ \frac{2\Omega_{F0} \ln [E_\Lambda^2(z)]}{E_\Lambda^2(z)} + \ln [E_\Lambda^2(z)]^2 \right\} \frac{b^2}{2} + \dots \end{aligned} \quad (64)$$

The second method  $M_2$  involves performing a Taylor expansion in the modified Friedman equation (57) directly. For the details in this case we refer the interested reader to the Appendix and just present the result here:

$$E^2(z, b) = -b \Omega_F \mathcal{W}_k \left( -\frac{e^{-\frac{E_\Lambda(z)^2}{b \Omega_F}}}{b \Omega_F} \right), \quad (65)$$

where  $\mathcal{W}_k(\omega)$  is the Lambert function defined via  $\omega \equiv \mathcal{W}_k(\omega)e^{\mathcal{W}_k(\omega)}$  for all complex numbers  $\omega$ . The Lambert function has branch-cut discontinuities, so the different branches are indicated by the integer  $k$ . Our solution has  $k = 0$  (the principal branch) for  $b \leq 0$  and  $k = -1$  for  $b > 0$ .<sup>2</sup>

In order to examine the accuracy of the approximations of (64) and (65), we calculate the average percent deviation from the exact numerical solution of (57), defined as

$$\langle \text{difference}(b) \rangle = \left\langle 100 \cdot \left( 1 - \frac{E_{\text{approx}}^2(z, b)}{E_{\text{numeric}}^2(z, b)} \right) \right\rangle, \quad (66)$$

where the average is taken over redshifts in the range  $z \in [0, 100]$ . In Fig. 1 we show the corresponding results. In particular, on the left plot we show the percent difference between the numerical solution of Eqs. (16) and (35) and the analytical approximations of Eqs. (64) and (65) as a function of  $z$ , for various values of the parameter  $b$  for both methods  $M_1$ , at first (dashed line) and second order (dotted line) and  $M_2$  (solid black line). As it can be seen, at redshifts  $z \lesssim 2$  method  $M_2$  is significantly

<sup>2</sup> The Lambert function  $\mathcal{W}_k(\omega)$  is defined in MATHEMATICA as ProductLog[ $k, \omega$ ] and can be evaluated to arbitrary precision for integer values of  $k$  and real or complex values of  $\omega$ .

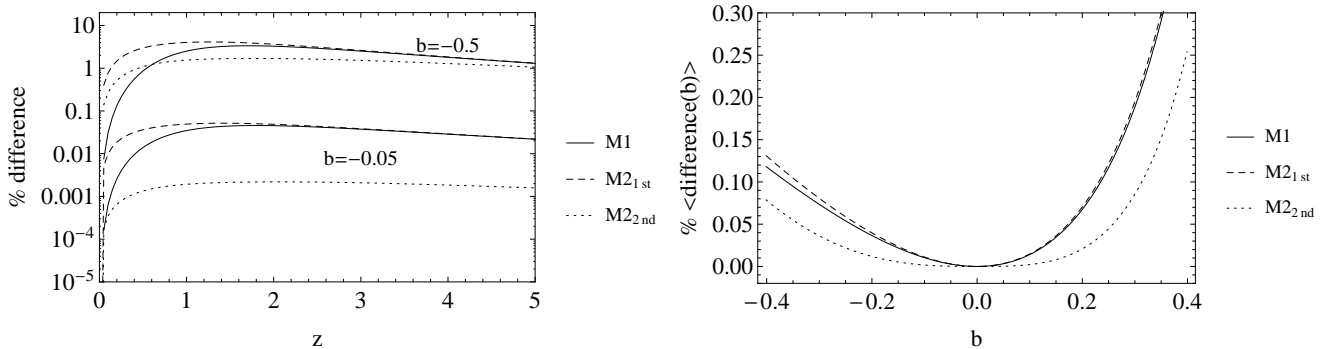


FIG. 1: Left: The percent difference( $z, b$ ) between the numerical solution of Eqs. (16) and (35) and the analytical approximations of Eqs. (64) and (65) as a function of  $z$ , for various values of the parameter  $b$  for both methods  $M_1$  (at first and second order) and  $M_2$ . Right: The average percent difference ( $\langle \text{difference}(b) \rangle$ ) between the numerical solution of Eqs. (16) and (35) and the analytical approximations of Eqs. (64) and (65) as a function of the parameter  $b$ . In this case, the average over the redshift is taken in the range  $z \in [0, 100]$ .

better than the first-order  $M_1$ , but overall, obviously the second-order method  $M_2$  is much better than the other two.

On the right plot we show the average percent difference ( $\langle \text{difference}(b) \rangle$ ) between the numerical solution of Eqs. (16) and (35) and the analytical approximations of Eqs. (64) and (65) as a function of the parameter  $b$ . In this case, the average over the redshift is taken in the range  $z \in [0, 100]$ . Clearly, on average the second-order method is significantly better than the other two methods, the first-order  $M_1$  and the  $M_2$ . Thus, we conclude that the second order series expansion of Eq. (64) around  $\Lambda$ CDM for the  $f_1$ CDM model is a very good approximation, especially for realistic values of the parameter  $b$ .

Unfortunately, for the  $f_2$ CDM and  $f_3$ CDM models it is not possible to analytically obtain similar expressions, due to the presence of terms like  $\sim e^{-1/b}$ , which do not admit a Taylor expansion around  $b \sim 0$ . However, as mentioned earlier, they both have the  $\Lambda$ CDM model as a limit for  $b \rightarrow 0^+$ .

## V. OBSERVATIONAL CONSTRAINTS

In this section we perform a complete and detailed observational analysis of the above five  $f(T)$  models. In particular, we implement a joint statistical analysis with the appropriate Akaike information criterion [52], involving the latest expansion data (SnIa [53], BAO [54, 55] and the 9-year WMAP CMB shift parameter [56]) and the growth data (as collected by [18]). The likelihood analysis, the Akaike information criterion, the expansion data, the growth data and the corresponding covariances can be found in Table I and Sec. IV of our previous work [18]. Moreover, we mention that since in order to deal with the growth data we need to know the value of  $\sigma_8$ , which is the rms mass fluctuation on  $R_8 = 8h^{-1}$  Mpc scales at redshift  $z = 0$ , we treat  $\sigma_8$  either as  $\sigma_8 = 0.8$  or as a free parameter. This analysis is significantly im-

proved, comparing to previous observational constraining of  $f(T)$  gravity [11, 15, 49, 51].

Let us now provide a presentation of our statistical results. In Table I we give the resulting best fit parameters for the various  $f(T)$  models under study (we impose here  $\sigma_8 = 0.8$ ), in which we also show the corresponding quantities for  $\Lambda$ CDM for comparison.

It is clear that utilizing the combination of the most recent growth data set with the expansion cosmological data, we can put tight constraints on  $(\Omega_m, \gamma)$ . In all cases the best fit value  $\Omega_m = 0.272 \pm 0.003$  is in a very good agreement with the one found by WMAP9+SPT+ACT, that is,  $\Omega_m = 0.272$  [56].

In particular, we find the following

(a)  $\Gamma_0$  parametrization. -

Regarding the  $\Lambda$ CDM cosmological model our best fit value growth is  $\gamma = 0.597 \pm 0.046$  that is in a good agreement with previous studies [18, 57–61]. Concerning the  $f(T)$  models we obtain  $(\gamma, b) = (0.602 \pm 0.052, -0.017 \pm 0.083)$ ,  $(\gamma, b) = (0.596 \pm 0.047, 0.121 \pm 0.184)$  and  $(\gamma, b) = (0.597 \pm 0.046, 0.097 \pm 0.155)$  for the  $f_1$ CDM,  $f_2$ CDM and  $f_3$ CDM models, respectively, with a reduced  $\chi^2_{min}$  of  $\sim 574.2$ . In Fig. 2 we show the  $1\sigma$ ,  $2\sigma$  and  $3\sigma$  confidence contours in the  $(\Omega_m, b)$  plane, while in Fig. 3 we present the corresponding contours in the  $(\Omega_m, \gamma)$  plane.

(b)  $\Gamma_1$  parametrization. -

In the case of the concordance  $\Lambda$  cosmology we find  $\gamma_0 = 0.567 \pm 0.066$  and  $\gamma_1 = 0.116 \pm 0.191$  with  $\chi^2_{min} \simeq 573.861$  which are in agreement with previous studies [18, 32, 59, 62, 63]. For the  $f_1$ CDM,  $f_2$ CDM and  $f_3$ CDM models the corresponding likelihood functions peak at  $(b, \gamma_0, \gamma_1) = (-0.029 \pm 0.088, 0.558 \pm 0.067, 0.187 \pm 0.205)$  with  $\chi^2_{min} \simeq 573.817$ ,  $(b, \gamma_0, \gamma_1) = (0.086 \pm 0.301, 0.566 \pm 0.066, 0.116 \pm 0.191)$  with  $\chi^2_{min} \simeq 573.863$  and  $(b, \gamma_0, \gamma_1) = (0.010 \pm 0.324, 0.570 \pm 0.067, 0.099 \pm 0.192)$  with  $\chi^2_{min} \simeq 573.852$ , respectively. In Fig. 4 we present the corresponding  $1\sigma$ ,  $2\sigma$  and  $3\sigma$  contours in the  $(\gamma_0, \gamma_1)$  plane.

(c)  $\Gamma_2$  parametrization. -

Exp. model	Param. model	$\Omega_{m0}$	$b$	$\gamma_0$	$\gamma_1$	$\chi^2_{min}$	AIC	$ \Delta AIC $
$\Lambda$ CDM	$\Gamma_0$	$0.272 \pm 0.003$		$0.597 \pm 0.046$	0	574.227	578.227	0
	$\Gamma_1$	$0.272 \pm 0.003$		$0.567 \pm 0.066$	$0.116 \pm 0.191$	573.861	579.861	1.634
	$\Gamma_2$	$0.272 \pm 0.003$		$0.561 \pm 0.068$	$0.183 \pm 0.269$	573.767	579.767	1.540
$f_1$ CDM [8]:	$\Gamma_0$	$0.274 \pm 0.008$	$-0.017 \pm 0.083$	$0.602 \pm 0.052$	0	574.203	580.203	1.976
	$\Gamma_1$	$0.275 \pm 0.008$	$-0.029 \pm 0.088$	$0.558 \pm 0.067$	$0.187 \pm 0.205$	573.817	581.817	3.590
	$\Gamma_2$	$0.275 \pm 0.008$	$-0.030 \pm 0.089$	$0.564 \pm 0.069$	$0.213 \pm 0.287$	573.640	581.640	3.413
$f_2$ CDM [9]:	$\Gamma_0$	$0.272 \pm 0.004$	$0.121 \pm 0.184$	$0.596 \pm 0.047$	0	574.250	580.250	2.023
	$\Gamma_1$	$0.272 \pm 0.003$	$0.086 \pm 0.301$	$0.566 \pm 0.066$	$0.116 \pm 0.191$	573.863	581.863	3.636
	$\Gamma_2$	$0.272 \pm 0.003$	$0.078 \pm 0.375$	$0.561 \pm 0.068$	$0.183 \pm 0.269$	573.768	581.768	3.541
$f_3$ CDM [48]:	$\Gamma_0$	$0.273 \pm 0.003$	$0.097 \pm 0.155$	$0.597 \pm 0.046$	0	574.223	580.223	1.996
	$\Gamma_1$	$0.273 \pm 0.003$	$0.010 \pm 0.324$	$0.570 \pm 0.067$	$0.099 \pm 0.192$	573.852	581.852	3.625
	$\Gamma_2$	$0.273 \pm 0.003$	$0.024 \pm 0.183$	$0.562 \pm 0.068$	$0.185 \pm 0.269$	573.749	581.749	3.522
$f_4$ CDM [49]:	$\Gamma_0$	$0.202 \pm 0.002$		$0.417 \pm 0.031$	0	704.481	708.481	130.254
	$\Gamma_1$	$0.202 \pm 0.002$		$0.468 \pm 0.053$	$-0.171 \pm 0.136$	702.865	708.865	130.638
	$\Gamma_2$	$0.202 \pm 0.002$		$0.467 \pm 0.052$	$-0.224 \pm 0.134$	703.047	709.047	130.820
$f_5$ CDM [51]:	$\Gamma_0$	$0.283 \pm 0.006$	$0.226 \pm 0.066$	$0.567 \pm 0.049$	0	579.583	585.583	7.356
	$\Gamma_1$	$0.277 \pm 0.006$	$0.298 \pm 0.049$	$0.550 \pm 0.065$	$0.099 \pm 0.191$	580.723	588.723	10.496
	$\Gamma_2$	$0.287 \pm 0.007$	$0.193 \pm 0.074$	$0.570 \pm 0.070$	$0.263 \pm 0.298$	578.027	586.027	7.800

TABLE I: Statistical results of the overall likelihood analysis: The first column indicates the  $f(T)$  model, the second column the  $\gamma(z)$  parametrizations appearing in Sec. III A, the third and fourth columns provide the  $\Omega_{m0}$  and  $b$  best values, and the fifth and sixth columns show the  $\gamma_0$  and  $\gamma_1$  best fit values. In all cases we have used  $\sigma_8 = 0.8$ . The last three columns present the goodness-of-fit statistics ( $\chi^2_{min}$ , AIC and  $|\Delta AIC| = |AIC_\Lambda - AIC_{f(T)}|$ ). All the error estimates come from the inverse of the Fisher matrix, called the covariance matrix, and are by definition symmetric.

In the case of  $\Lambda$ CDM model we have  $\gamma_0 = 0.561 \pm 0.068$ ,  $\gamma_1 = 0.183 \pm 0.269$  ( $\chi^2_{min} \simeq 573.767$ ), while for the  $f_1$ CDM we obtain  $b = -0.030 \pm 0.089$ ,  $\gamma_0 = 0.564 \pm 0.069$ ,  $\gamma_1 = 0.213 \pm 0.287$  ( $\chi^2_{min} \simeq 573.640$ ), for the  $f_2$ CDM gravity model we find  $b = 0.150 \pm 0.096$ ,  $\gamma_0 = 0.560 \pm 0.068$ ,  $\gamma_1 = 0.181 \pm 0.271$  ( $\chi^2_{min} \simeq 573.921$ ) and finally for the  $f_3$ CDM model we have we find  $b = 0.024 \pm 0.183$ ,  $\gamma_0 = 0.562 \pm 0.068$ ,  $\gamma_1 = 0.185 \pm 0.269$  ( $\chi^2_{min} \simeq 573.749$ ). In Fig. 5 we present the corresponding  $1\sigma$ ,  $2\sigma$  and  $3\sigma$  contours in the  $(\gamma_0, \gamma_1)$  plane.

We stress here that in all three previous  $f(T)$  models, namely,  $f_{1-3}$ CDM ones, the parameter  $b$  which quantifies the deviation from  $\Lambda$ CDM cosmology is constrained in a very narrow window around 0. Thus, although these three models are consistent with observations, their viable forms are practically indistinguishable from  $\Lambda$ CDM and therefore their new degrees of freedom are disfavored by data.

Finally, in Fig. 6 we show the likelihood contours for  $f_4$ CDM model, which as discussed in Sec. IV coincides with DGP at the background level, and thus it shares its observational disadvantages and therefore we consider it as nonviable. In the same lines, as we can see from Table I, for  $f_5$ CDM model we obtain the best fits  $\chi^2_{min} = (579.583, 580.723, 578.027)$  for the  $\Gamma_0$ ,  $\Gamma_1$  and  $\Gamma_2$  growth-rate parameterizations respectively, while it additionally has one more free parameter than  $\Lambda$ CDM. Thus, this

model is in tension with the data.

For completeness, in Figs. 7-9 we present a comparison of the observed and theoretical evolution of the growth rate  $f\sigma_8(z) = F(z)\sigma_8(z)$ , the evolution of the growth index  $\gamma(z) - \frac{6}{11}$  and the evolution of the  $G_{\text{eff}}(z)$  respectively.

Finally, in order to enhance the validity of the above results, we repeat the whole analysis by using  $\sigma_8$  as a free parameter. As expected, we find that the corresponding results are in good agreement, within  $1\sigma$ , with those of  $\sigma_8 = 0.8$  (see Table I). In particular, we find the following.

In the case of the  $\Lambda$ CDM,

- for the  $\Gamma_0$  model:  $\chi^2 = 573.254$ ,  $\Omega_m = 0.272 \pm 0.003$ ,  $\gamma_0 = 0.523 \pm 0.0858$ ,  $\sigma_8 = 0.761 \pm 0.038$ ;
- for the  $\Gamma_1$  model:  $\chi^2 = 572.618$ ,  $\Omega_m = 0.272 \pm 0.003$ ,  $\gamma_0 = 0.485 \pm 0.098$ ,  $\gamma_1 = -0.398 \pm 0.502$ ,  $\sigma_8 = 0.694 \pm 0.087$ ;
- for the  $\Gamma_2$  model:  $\chi^2 = 572.652$ ,  $\Omega_m = 0.272 \pm 0.003$ ,  $\gamma_0 = 0.483 \pm 0.097$ ,  $\gamma_1 = -0.633 \pm 0.815$ ,  $\sigma_8 = 0.685 \pm 0.097$ ;

In the case of the  $f_1$ CDM,

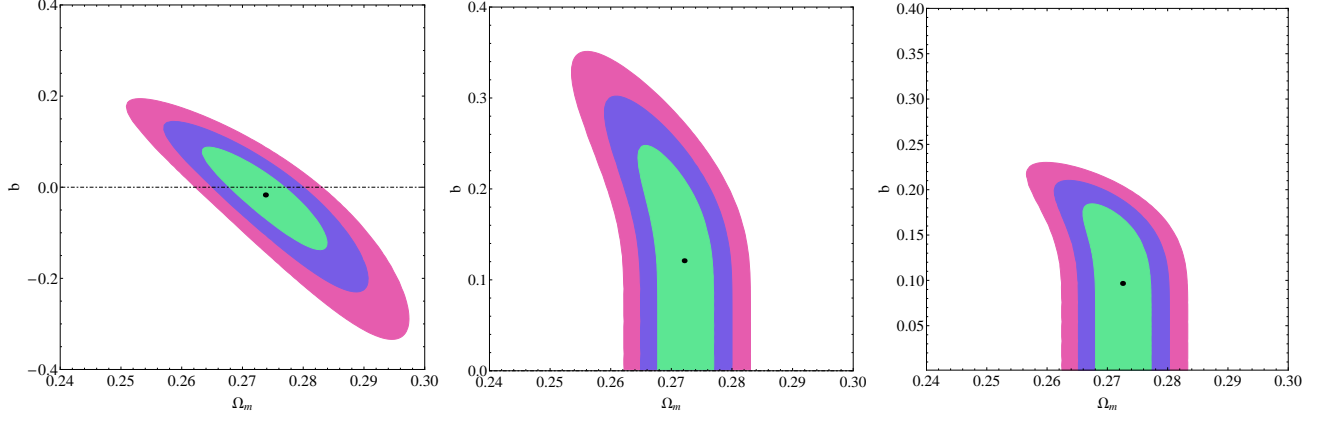


FIG. 2: Likelihood contours for  $\delta\chi^2 \equiv \chi^2 - \chi^2_{min}$  equal to 2.30, 6.18 and 11.83, corresponding to  $1\sigma$ ,  $2\sigma$  and  $3\sigma$  confidence levels, in the  $(\Omega_m, b)$  plane for the  $\Gamma_0$  growth rate parametrization and the  $f_1$ CDM (left),  $f_2$ CDM (middle) and  $f_3$ CDM (right) models. In all cases the black point corresponds to the best fit. In this plot and in the ones that follow we have set the parameters that are not shown to their best fit values for the corresponding model (see Table I).

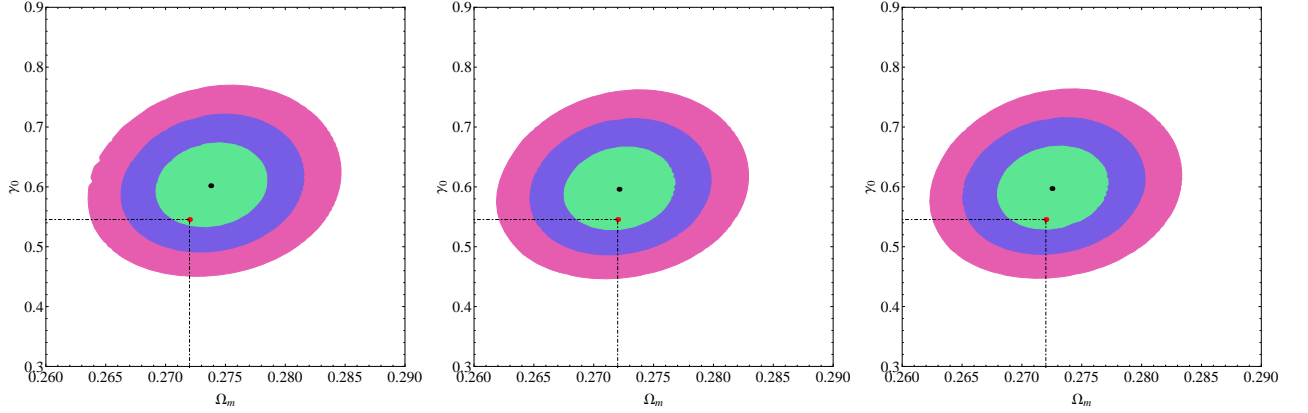


FIG. 3: Likelihood contours for  $\delta\chi^2 \equiv \chi^2 - \chi^2_{min}$  equal to 2.30, 6.18 and 11.83, corresponding to  $1\sigma$ ,  $2\sigma$  and  $3\sigma$  confidence levels, in the  $(\Omega_m, \gamma_0)$  plane for the  $\Gamma_0$  growth rate parametrization and the  $f_1$ CDM (left),  $f_2$ CDM (middle) and  $f_3$ CDM (right) models. In all cases the red point corresponds to  $(\Omega_m, \gamma_0) = (0.272, 6/11)$ .

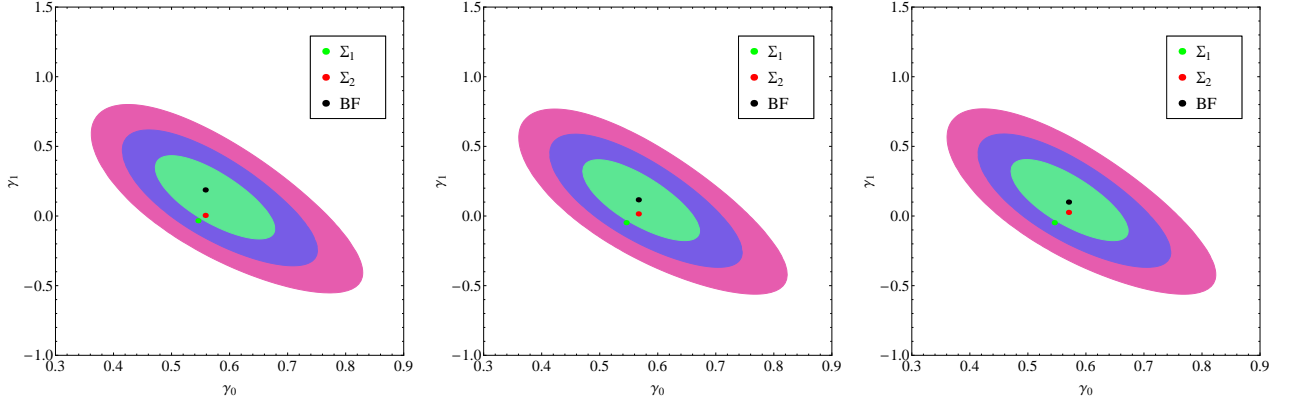


FIG. 4: Likelihood contours for  $\delta\chi^2 \equiv \chi^2 - \chi^2_{min}$  equal to 2.30, 6.18 and 11.83, corresponding to  $1\sigma$ ,  $2\sigma$  and  $3\sigma$  confidence levels, in the  $(\gamma_0, \gamma_1)$  plane for the  $\Gamma_1$  growth rate parametrization and for the  $f_1$ CDM (left),  $f_2$ CDM (middle) and  $f_3$ CDM (right) models. We also include the theoretical  $\Lambda$ CDM  $(\gamma_0, \gamma_1)$  values given by  $\Sigma_1 = (6/11, \gamma_1(6/11, \Omega_{m0,bf}))$  and  $\Sigma_2 = (\gamma_{0,bf}, \gamma_1(\gamma_{0,bf}, \Omega_{m0,bf}))$ .

• for the  $\Gamma_0$  model:  $\chi^2 = 573.618$ ,  $\Omega_m = 0.274 \pm 0.008$ ,  $b = -0.019 \pm 0.087$ ,  $\gamma_0 = 0.586 \pm 0.090$ ,

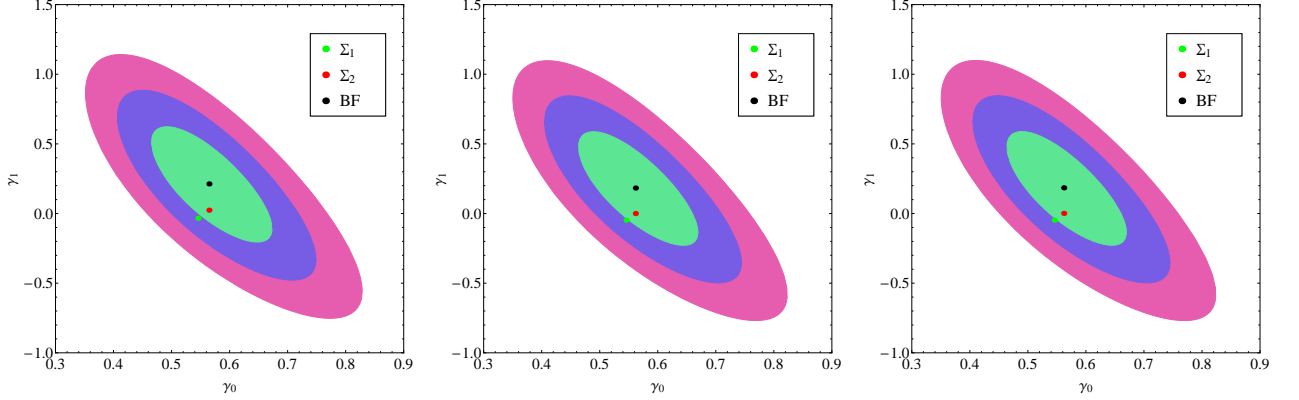


FIG. 5: Likelihood contours for  $\delta\chi^2 \equiv \chi^2 - \chi_{min}^2$  equal to 2.30, 6.18 and 11.83, corresponding to  $1\sigma$ ,  $2\sigma$  and  $3\sigma$  confidence levels, in the  $(\gamma_0, \gamma_1)$  plane for the  $\Gamma_2$  growth rate parametrization and for the  $f_1$ CDM (left),  $f_2$ CDM (middle) and  $f_3$ CDM (right) models. We also include the theoretical  $\Lambda$ CDM  $(\gamma_0, \gamma_1)$  values given by  $\Sigma_1 = (6/11, \gamma_1(6/11, \Omega_{m0,bf}))$  and  $\Sigma_2 = (\gamma_{0,bf}, \gamma_1(\gamma_{0,bf}, \Omega_{m0,bf}))$ .

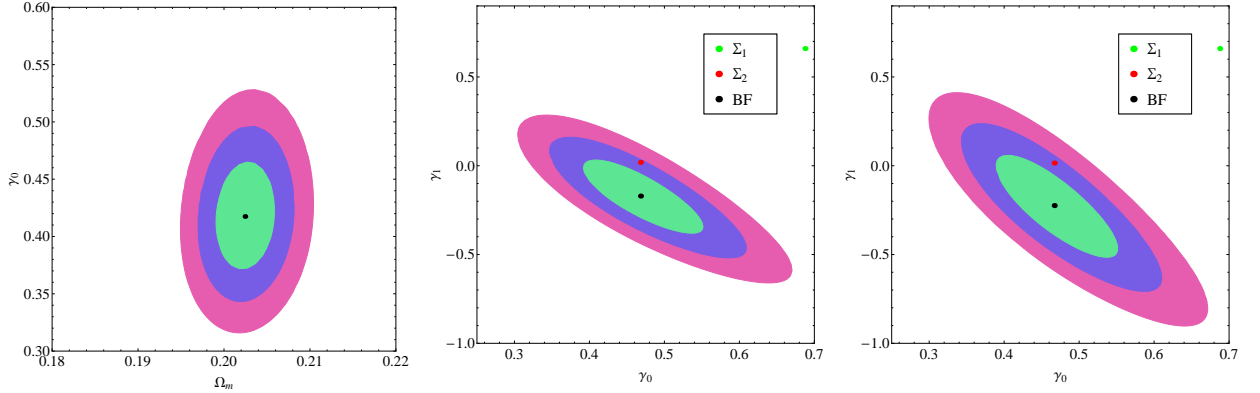


FIG. 6: Likelihood contours for  $\delta\chi^2 \equiv \chi^2 - \chi_{min}^2$  equal to 2.30, 6.18 and 11.83, corresponding to  $1\sigma$ ,  $2\sigma$  and  $3\sigma$  confidence levels, for the  $f_4$ CDM model in the  $(\Omega_m, \gamma_0)$  plane (left) and the  $(\gamma_0, \gamma_1)$  plane (middle) and (right). We also include the theoretical  $\Lambda$ CDM  $(\gamma_0, \gamma_1)$  values given by  $\Sigma_1 = (11/16, \gamma_1(11/16, \Omega_{m0,bf}))$  (with the value  $\gamma_0 = 11/16$  corresponding to the DGP) and  $\Sigma_2 = (\gamma_{0,bf}, \gamma_1(\gamma_{0,bf}, \Omega_{m0,bf}))$ . As was mentioned in the text, the difference between the DGP (green point) and  $f_4$ CDM (black point) is due to the different  $G_{eff}(z)$ , which affects the evolution of the matter density perturbations.

$$\sigma_8 = 0.783 \pm 0.041;$$

- for the  $\Gamma_1$  model:  $\chi^2 = 576.124$ ,  $\Omega_m = 0.281 \pm 0.009$ ,  $b = -0.099 \pm 0.109$ ,  $\gamma_0 = 0.582 \pm 0.092$ ,  $\gamma_1 = 0.680 \pm 0.443$ ,  $\sigma_8 = 0.752 \pm 0.070$ ;
- for the  $\Gamma_2$  model:  $\chi^2 = 573.756$ ,  $\Omega_m = 0.281 \pm 0.008$ ,  $b = -0.098 \pm 0.104$ ,  $\gamma_0 = 0.569 \pm 0.103$ ,  $\gamma_1 = 0.077 \pm 0.872$ ,  $\sigma_8 = 0.774 \pm 0.114$ ;

In the case of the  $f_2$ CDM,

- for the  $\Gamma_0$  model:  $\chi^2 = 573.264$ ,  $\Omega_m = 0.272 \pm 0.003$ ,  $b = 0.101 \pm 0.186$ ,  $\gamma_0 = 0.523 \pm 0.086$ ,  $\sigma_8 = 0.762 \pm 0.038$ ;
- for the  $\Gamma_1$  model:  $\chi^2 = 572.618$ ,  $\Omega_m = 0.272 \pm 0.003$ ,  $b = 0.052 \pm 2.833$ ,  $\gamma_0 = 0.485 \pm 0.098$ ,  $\gamma_1 = -0.398 \pm 0.502$ ,  $\sigma_8 = 0.694 \pm 0.087$ ;

- for the  $\Gamma_2$  model:  $\chi^2 = 572.817$ ,  $\Omega_m = 0.272 \pm 0.003$ ,  $b = 0.040 \pm 10.476$ ,  $\gamma_0 = 0.500 \pm 0.113$ ,  $\gamma_1 = -0.599 \pm 1.022$ ,  $\sigma_8 = 0.699 \pm 0.127$ ;

In the case of the  $f_3$ CDM,

- for the  $\Gamma_0$  model:  $\chi^2 = 573.224$ ,  $\Omega_m = 0.273 \pm 0.003$ ,  $b = 0.050 \pm 2.561$ ,  $\gamma_0 = 0.523 \pm 0.086$ ,  $\sigma_8 = 0.761 \pm 0.038$ ;
- for the  $\Gamma_1$  model:  $\chi^2 = 572.599$ ,  $\Omega_m = 0.273 \pm 0.003$ ,  $b = 0.051 \pm 2.264$ ,  $\gamma_0 = 0.485 \pm 0.098$ ,  $\gamma_1 = -0.398 \pm 0.502$ ,  $\sigma_8 = 0.694 \pm 0.087$ ;
- for the  $\Gamma_2$  model:  $\chi^2 = 572.636$ ,  $\Omega_m = 0.273 \pm 0.003$ ,  $b = 0.039 \pm 4.180$ ,  $\gamma_0 = 0.486 \pm 0.098$ ,  $\gamma_1 = -0.598 \pm 0.817$ ,  $\sigma_8 = 0.688 \pm 0.098$ ;

In the case of the  $f_4$ CDM,

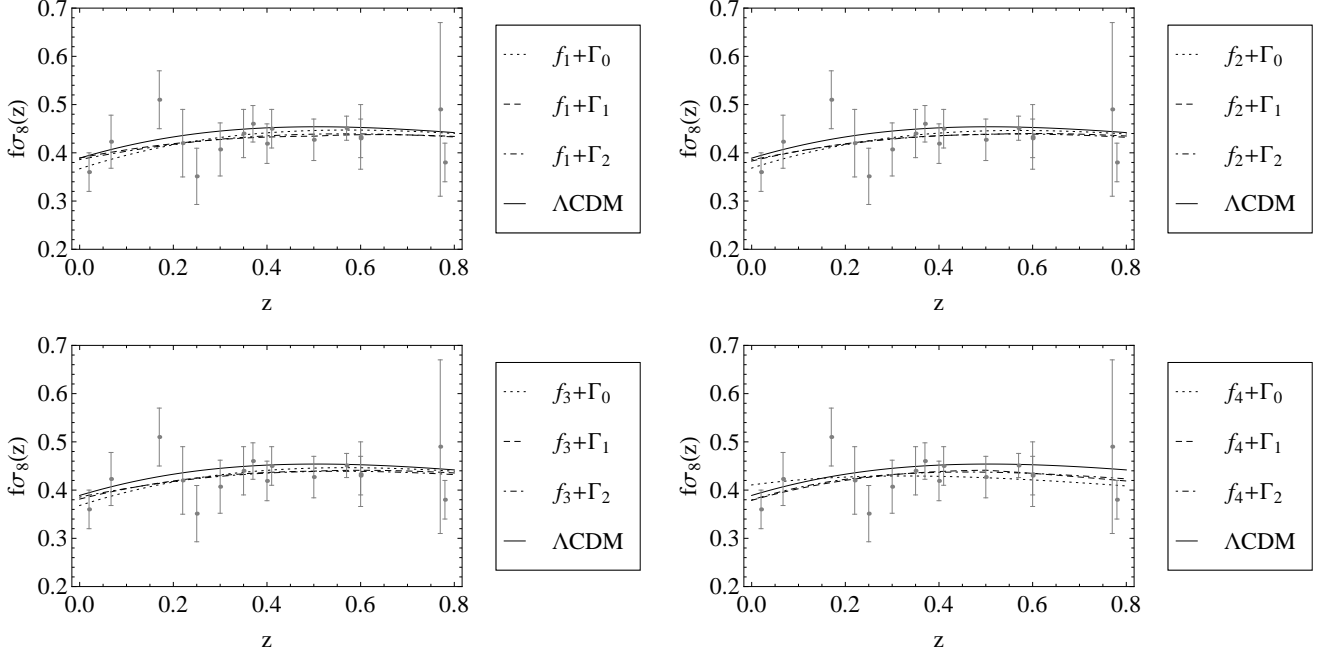


FIG. 7: Comparison of the observed and theoretical evolution of the growth rate  $f\sigma_8(z) = F(z)\sigma_8(z)$  for the  $f_{1-4}$ CDM models [ $f_1$ CDM (top left),  $f_2$ CDM (top right),  $f_3$ CDM (bottom left),  $f_4$ CDM (bottom right)] and the various growth rate parameterizations. The dotted, dashed and dot-dashed lines correspond to the best fit  $\Gamma_0$ ,  $\Gamma_1$  and  $\Gamma_2$  parameterizations while the solid black line corresponds to the exact solution of Eq. (19) for  $f\sigma_8(z)$  for the  $\Lambda$ CDM model for  $\Omega_m = 0.273$  [56].

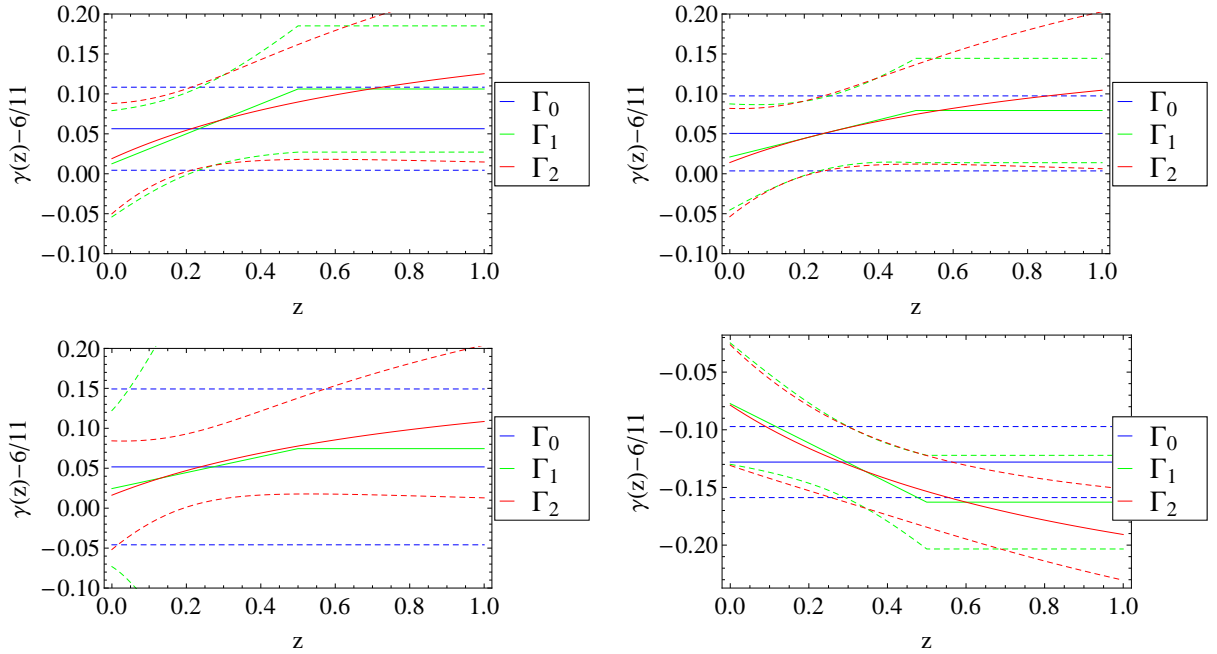


FIG. 8: The evolution of the growth index  $\gamma(z) - \frac{6}{11}$  for the  $f_{1-4}$ CDM models [ $f_1$ CDM (top left),  $f_2$ CDM (top right),  $f_3$ CDM (bottom left),  $f_4$ CDM (bottom right)] and the various growth rate parameterizations. The lines correspond to  $\Gamma_0$  (blue),  $\Gamma_1$  (green), and  $\Gamma_2$  (red).

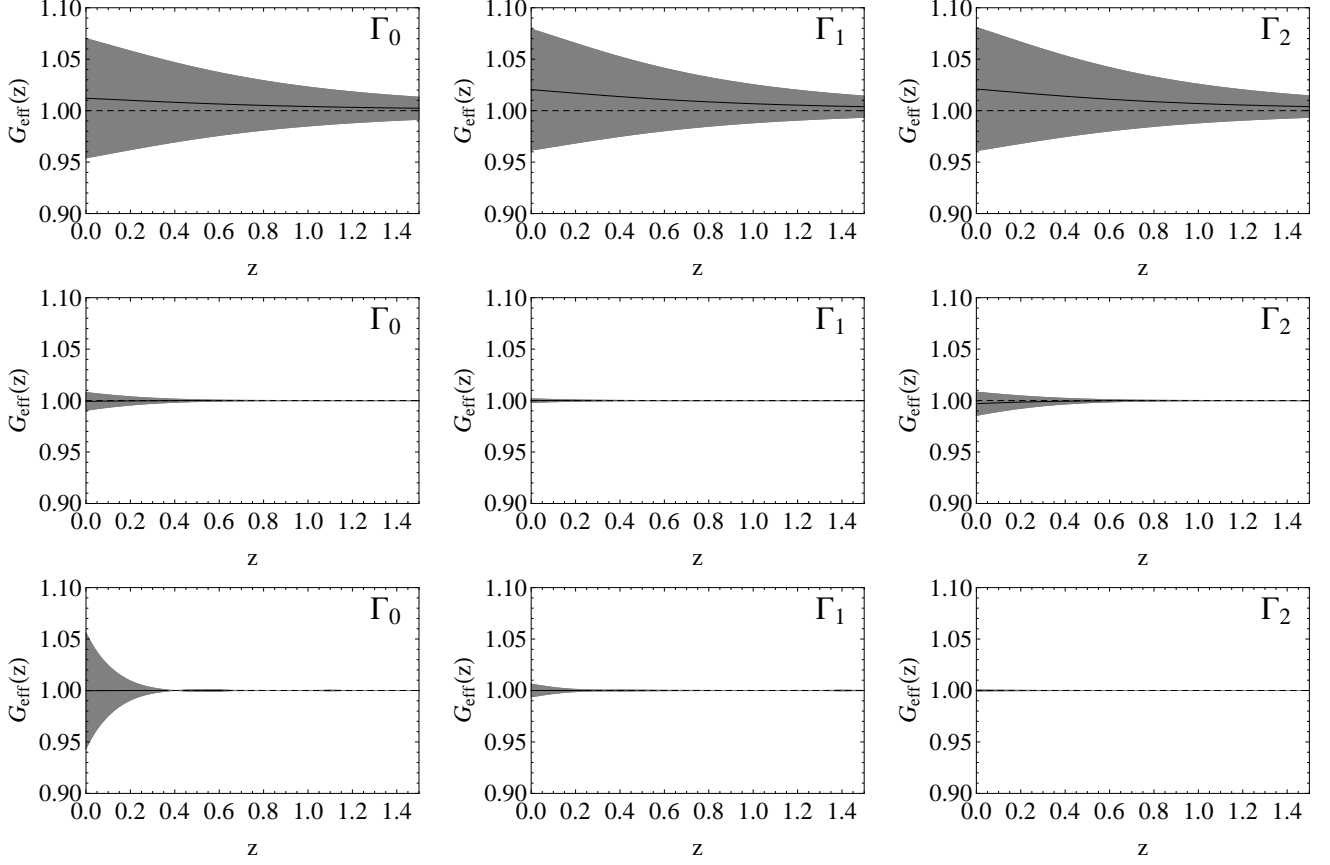


FIG. 9: The evolution of the  $G_{\text{eff}}(z)$  for the  $f_{1-3}$ CDM models and the various growth rate parameterizations considered in the text,  $f_1$ CDM (top),  $f_2$ CDM (middle),  $f_3$ CDM (bottom), for all three growth rate parameterizations  $\Gamma_0$  (left),  $\Gamma_1$  (middle), and  $\Gamma_2$  (right). The remarkable agreement between  $G_{\text{eff}}(z)$  and unity for the  $f_2$ CDM and  $f_3$ CDM models is easily explained by the fact that these models exhibit little deviation from  $\Lambda$ CDM, as is easily seen in Table I.

- for the  $\Gamma_0$  model:  $\chi^2 = 703.539$ ,  $\Omega_m = 0.202 \pm 0.002$ ,  $\gamma_0 = 0.490 \pm 0.083$ ,  $\sigma_8 = 0.856 \pm 0.061$ ;
- for the  $\Gamma_1$  model:  $\chi^2 = 702.419$ ,  $\Omega_m = 0.202 \pm 0.002$ ,  $\gamma_0 = 0.399 \pm 0.113$ ,  $\gamma_1 = -0.418 \pm 0.401$ ,  $\sigma_8 = 0.703 \pm 0.134$ ;
- for the  $\Gamma_2$  model:  $\chi^2 = 702.501$ ,  $\Omega_m = 0.202 \pm 0.002$ ,  $\gamma_0 = 0.379 \pm 0.123$ ,  $\gamma_1 = -0.733 \pm 0.713$ ,  $\sigma_8 = 0.667 \pm 0.154$ ;

In the case of the  $f_5$ CDM,

- for the  $\Gamma_0$  model:  $\chi^2 = 577.279$ ,  $\Omega_m = 0.285 \pm 0.006$ ,  $b = 0.217 \pm 0.067$ ,  $\gamma_0 = 0.550 \pm 0.086$ ,  $\sigma_8 = 0.765 \pm 0.038$ ;
- for the  $\Gamma_1$  model:  $\chi^2 = 577.176$ ,  $\Omega_m = 0.287 \pm 0.007$ ,  $b = 0.189 \pm 0.076$ ,  $\gamma_0 = 0.524 \pm 0.092$ ,  $\gamma_1 = 0.057 \pm 0.470$ ,  $\sigma_8 = 0.758 \pm 0.083$ ;
- for the  $\Gamma_2$  model:  $\chi^2 = 575.983$ ,  $\Omega_m = 0.287 \pm 0.007$ ,  $b = 0.189 \pm 0.076$ ,  $\gamma_0 = 0.489 \pm 0.090$ ,  $\gamma_1 = -0.717 \pm 0.743$ ,  $\sigma_8 = 0.674 \pm 0.078$ .

Lastly, we would like to emphasize that in all cases explored here the value of  $\text{AIC}_\Lambda$  ( $\sim 578.3$ ) is smaller than the corresponding one for the various  $f(T)$  models, which implies that the usual  $\Lambda$ CDM cosmology ( $\gamma_\Lambda = 0.597$ ) seems to provide a better fit than the  $f_{1-3}$ CDM gravity models the expansion and the growth data. On the other hand, the  $|\Delta\text{AIC}| = |\text{AIC}_\Lambda - \text{AIC}_{f_{1-3}(T)}|$  values point that the growth data can be consistent with the  $f_{1-3}$ CDM gravity models. We stress here that the  $f_4$ CDM and  $f_5$ CDM models seem to be disfavored by the current data.

## VI. DISCUSSION AND CONCLUSIONS

We have investigated a wide range of different  $f(T)$  models, with up to two parameters, both at the background and at the perturbation level. The functional forms of  $f(T)$  considered in this work cover practically all the functional forms considered in the literature so far. Despite the fact that the  $f(T)$  gravity can be derived from the principle of least action the corresponding  $f(T)$  functional forms are phenomenological and even though

they do not correspond to a firm theoretical model they cover a wide range of independent functional forms. Thus they represent a wide range of degrees of freedom describing deviations from  $\Lambda$ CDM in the context of  $f(T)$  models.

Following our previous work Basilakos, Nesseris and Perivolaropoulos [18] corresponding to  $f(R)$  gravity, we calculated the function  $y(z, b)$  which quantifies the deviation from  $\Lambda$ CDM cosmology at the background level. We also obtained the growth index and the effective Newton constant, which incorporate the  $f(T)$  gravity effects at the perturbation level. Furthermore, we utilized the recent expansion and growth data, implementing the Akaike information criterion and three different parametrizations for the growth index, in order to constraint the parameters of these  $f(T)$  models.

Our results show that all viable  $f(T)$  gravity models hardly deviate from the  $\Lambda$ CDM paradigm. In particular, among the five examined models, the power-law one [8] ( $f_1$ CDM), the exponential-square-root one [9] ( $f_2$ CDM) and the exponential one ( $f_3$ CDM) possess  $\Lambda$ CDM cosmology as a limiting case. It is only this limit that is favored by cosmological observations. In fact, the detailed observational confrontation showed that these three models at best fit, behave as small perturbations around the concordance  $\Lambda$ CDM cosmology, with the parameter  $b$ , which quantifies the deviation from  $\Lambda$ CDM, constrained in a very narrow window around 0. The other two  $f(T)$  models, namely the logarithmic one [49] ( $f_4$ CDM) and the hyperbolic-tangent one [51] ( $f_5$ CDM), do not possess  $\Lambda$ CDM as a limiting case. We showed that both are in tension with the data. In fact, we have demonstrated that ( $f_4$ CDM) coincides with the DGP model at the background level, whose inconsistency between distance measures and horizon scale growth is well known [50] and also demonstrated by our results.

The derived requirement of fine-tuning of the  $f(T)$  constructions at the  $\Lambda$ CDM, based on cosmological constraints, would probably be further amplified if we had considered in addition their consistency with Solar System tests, which constitute another powerful source of constraints against any deviation from general relativity. At this point we would like to make a comment concerning the Lorentz invariance of  $f(T)$  theories. As was shown in [64], for general  $f(T)$  modifications the field equations are not invariant under local Lorentz transformations, unless  $f(T)$  is a constant or a linear-in- $T$  function, in which case we reobtain general relativity (that is,  $\Lambda$ CDM) and local Lorentz invariance is restored. This feature imposes strict constraints on the viable  $f(T)$  forms, since the observational bounds on gravitational Lorentz violation are very narrow [65]. As we have already mentioned above, confrontation with Solar System data implies that the nontrivial  $f(T)$  modification must be significantly small [13]. In the present analysis we were interested in performing a pure confrontation of  $f(T)$  theories with cosmological data, without imposing any other theoretical constraints. Thus, from another

point of view we verified again that in all viable  $f(T)$  scenarios the nontrivial  $f(T)$  modifications are so small that these constructions are practically indistinguishable from  $\Lambda$ CDM. Clearly, taking into account the above Lorentz violation discussion strengthens our result that all viable  $f(T)$  almost coincide with  $\Lambda$ CDM.

It is therefore safe to conclude that although at early times the additional degrees of freedom provided by  $f(T)$  constructions may play an important role and improve the inflationary behavior, at late times these extra degrees of freedom do not appear to be consistent with the degrees of freedom favored by nature.

### Acknowledgements

The authors would like to thank Q.-G.Huang and C.-C. Lee for useful comments. S.B. acknowledges support by the Research Center for Astronomy of the Academy of Athens in the context of the program “*Tracing the Cosmic Acceleration*”. S.N. acknowledges financial support from the Madrid Regional Government (CAM) under the program HEPHACOS S2009/ESP-1473-02, from MICINN under Grant No. AYA2009-13936-C06-06 and Consolider-Ingenio 2010 PAU (CSD2007-00060), as well as from the European Union Marie Curie Initial Training Network UNILHC PITN-GA-2009-237920. S.N. also acknowledges the support of the Spanish MINECO’s “Centro de Excelencia Severo Ochoa” Programme under Grant No. SEV-2012-0249. The research of E.N.S. is implemented within the framework of the Action “Supporting Postdoctoral Researchers” of the Operational Program “Education and Lifelong Learning” Actionâs Beneficiary: (General Secretariat for Research and Technology), and is cofinanced by the European Social Fund (ESF) and the Greek State. This research has been cofinanced by the European Union (European Social Fund - ESF) and Greek national funds through the Operational Program ”Education and Lifelong Learning” of the National Strategic Reference Framework (NSRF) - Research Funding Program: THALIS. Investing in the society of knowledge through the European Social Fund.

### Appendix A: DERIVATION OF EQ. (65)

We can rewrite Eq. (57) as

$$\begin{aligned} E^2(z) &= \Omega_{m0}(1+z)^3 + \Omega_{r0}(1+z)^4 + \Omega_{F0}E^{2b}(z) \\ &= \Omega_{m0}(1+z)^3 + \Omega_{r0}(1+z)^4 + \Omega_{F0} - \Omega_{F0} \\ &\quad + \Omega_{F0}E^{2b}(z) \\ &= E_{\Lambda}^2(z) + \Omega_{F0} [E^{2b}(z) - 1], \end{aligned} \quad (A1)$$

where  $E_{\Lambda}^2(z)$  is given by Eq. (59) and in the second line we added and subtracted  $\Omega_{F0}$ .

Now, in this case we assume that the Hubble parameter  $\frac{H^2}{H_0^2} \equiv E^2(z)$  depends on  $b$  only implicitly via the Friedmann equation (59). In other words, we consider  $b$  and  $E^2(z)$  to be independent, and thus any derivatives with respect to  $b$  are zero. Hence, performing a Taylor expansion of (A1) up to second order around  $b = 0$  we acquire

$$E^2(z) = E_\Lambda^2(z) + \ln[E^2(z)] \Omega_{F0} b + \frac{1}{2} \ln[E^2(z)]^2 \Omega_{F0} b^2 + \dots \quad (\text{A2})$$

If we keep only the first-order term and solve for  $E^2(z)$ ,

we obtain

$$E^2(z, b) = -b \Omega_{F0} \mathcal{W}_k \left( -\frac{e^{-\frac{E_\Lambda(z)^2}{b \Omega_{F0}}}}{b \Omega_{F0}} \right), \quad (\text{A3})$$

where  $\mathcal{W}_k(\omega)$  is the Lambert function defined via  $\omega \equiv \mathcal{W}_k(\omega)e^{\mathcal{W}_k(\omega)}$  for all complex numbers  $\omega$ . The Lambert function has branch-cut discontinuities, so the different branches are indicated by the integer  $k$ . Our solution has  $k = 0$  (the principal branch) for  $b \leq 0$  and  $k = -1$  for  $b > 0$ .

- 
- [1] S. Capozziello and M. De Laurentis, Phys. Rept. **509**, 167 (2011).
- [2] E. J. Copeland, M. Sami and S. Tsujikawa, Intern. Journal of Modern Physics D, **15**, 1753,(2006); R. R. Caldwell and M. Kamionkowski, Ann.Rev.Nucl.Part.Sci., **59**, 397 (2009); I. Sawicki and W. Hu, Phys. Rev. D, **75**, 127502 (2007).
- [3] L. Amendola and S. Tsujikawa, *Dark Energy Theory and Observations*, Cambridge University Press, Cambridge UK, (2010).
- [4] A. Einstein, Sitz. Preuss. Akad. Wiss. p. **17**, 217 (1928); **17** 224 (1928); A. Unzicker and T. Case, physics/0503046.
- [5] K. Hayashi and T. Shirafuji, Phys. Rev. D **19**, 3524 (1979); Addendum-ibid. **24**, 3312 (1981).
- [6] J. W. Maluf, J. Math. Phys. **35** (1994) 335; H. I. Arcos and J. G. Pereira, Int. J. Mod. Phys. D **13**, 2193 (2004).
- [7] R. Ferraro and F. Fiorini, Phys. Rev. D **75**, 084031 (2007); R. Ferraro, F. Fiorini, Phys. Rev. **D78**, 124019 (2008).
- [8] G. R. Bengochea, & R. Ferraro, Phys. Rev. D, **79**, 124019, (2009).
- [9] E. V. Linder, Phys. Rev. D **81**, 127301 (2010); Erratum, Phys. Rev. D, **82**, 109902.
- [10] K. K. Yerzhanov, S. .R. Myrzakul, I. I. Kulnazarov and R. Myrzakulov, arXiv:1006.3879 [gr-qc]; K. Bamba, C. -Q. Geng and C. -C. Lee, arXiv:1008.4036 [astro-ph.CO]; R. -J. Yang, Europhys. Lett. **93**, 60001 (2011); Y. Zhang, H. Li, Y. Gong, Z. -H. Zhu, JCAP **1107**, 015 (2011); R. Ferraro, F. Fiorini, Phys. Lett. **B702**, 75 (2011). Y. -F. Cai, S. -H. Chen, J. B. Dent, S. Dutta, E. N. Saridakis, Class. Quant. Grav. **28**, 2150011 (2011); M. Sharif, S. Rani, Mod. Phys. Lett. **A26**, 1657 (2011); S. Capozziello, V. F. Cardone, H. Farajollahi and A. Ravanpak, Phys. Rev. D **84**, 043527 (2011); K. Bamba and C. -Q. Geng, JCAP **1111**, 008 (2011); C. -Q. Geng, C. -C. Lee, E. N. Saridakis, Y. -P. Wu, Phys. Lett. **B704**, 384 (2011); H. Wei, Phys. Lett. B **712**, 430 (2012); C. -Q. Geng, C. -C. Lee, E. N. Saridakis, JCAP **1201**, 002 (2012); Y. -P. Wu and C. -Q. Geng, Phys. Rev. D **86**, 104058 (2012); C. G. Bohmer, T. Harko and F. S. N. Lobo, Phys. Rev. D **85**, 044033 (2012); H. Farajollahi, A. Ravanpak and P. Wu, Astrophys. Space Sci. **338**, 23 (2012); K. Atazadeh and F. Darabi, Eur. Phys. J. C **72**, 2016 (2012); M. Jamil, D. Momeni, N. S. Serikbayev and R. Myrzakulov, Astrophys. Space Sci. **339**, 37 (2012); J. Yang, Y. -L. Li, Y. Zhong and Y. Li, arXiv:1202.0129 [hep-th]; K. Karami and A. Abdolmaleki, JCAP **1204**, 007 (2012); C. Xu, E. N. Saridakis and G. Leon, JCAP **1207**, 005 (2012); K. Bamba, R. Myrzakulov, S. 'i. Nojiri and S. D. Odintsov, arXiv:1202.4057 [physics.gen-ph]; D. Liu, P. Wu and H. Yu, Int. J. Mod. Phys. D **21**, 1250074 (2012); H. Dong, Y. -b. Wang and X. -h. Meng, Eur. Phys. J. C **72**, 2002 (2012); N. Tamanini and C. G. Boehmer, Phys. Rev. D **86**, 044009 (2012); K. Bamba, S. Capozziello, S. 'i. Nojiri and S. D. Odintsov, Astrophys. Space Sci. **342**, 155 (2012); A. Behboodi, S. Akhshabi and K. Nozari, Phys. Lett. B **718**, 30 (2012); A. Banijamali and B. Fazlpour, Astrophys. Space Sci. **342**, 229 (2012); D. Liu and M. J. Reboucas, Phys. Rev. D **86**, 083515 (2012); M. E. Rodrigues, M. J. S. Houndjo, D. Saez-Gomez and F. Rahaman, Phys. Rev. D **86**, 104059 (2012); Y. -P. Wu and C. -Q. Geng, arXiv:1211.1778 [gr-qc]; S. Chattopadhyay and A. Pasqua, Astrophys. Space Sci. **344**, 269 (2013); M. Jamil, D. Momeni and R. Myrzakulov, Gen. Rel. Grav. **45**, 263 (2013); K. Bamba, J. de Haro and S. D. Odintsov, JCAP **1302**, 008 (2013); M. Jamil, D. Momeni and R. Myrzakulov, Eur. Phys. J. C **72**, 2267 (2012); J. -T. Li, C. -C. Lee and C. -Q. Geng, Eur. Phys. J. C **73**, 2315 (2013); H. M. Sadjadi, Phys. Rev. D **87**, 064028 (2013); A. Aviles, A. Bravetti, S. Capozziello and O. Luongo, Phys. Rev. D **87**, 064025 (2013); Y. C. Ong, K. Izumi, J. M. Nester and P. Chen, Phys. Rev. D **88**, 024019 (2013); K. Bamba, S. 'i. Nojiri and S. D. Odintsov, arXiv:1304.6191 [gr-qc]; H. Dong, J. Wang and X. Meng, arXiv:1304.6587 [gr-qc]; G. Otalora, JCAP **1307**, 044 (2013); J. Amoros, J. de Haro and S. D. Odintsov, Phys. Rev. D **87**, 104037 (2013); F. Darabi, arXiv:1305.5378 [gr-qc]; G. Otalora, arXiv:1305.5896 [gr-qc]; C. -Q. Geng, J. -A. Gu and C. -C. Lee, Phys. Rev. D **88**, 024030 (2013); I. G. Salako, M. E. Rodrigues, A. V. Kpadonou, M. J. S. Houndjo and J. Tossa, arXiv:1307.0730 [gr-qc]; A. V. Astashenok, arXiv:1308.0581 [gr-qc]; M. E. Rodrigues, I. G. Salako, M. J. S. Houndjo and J. Tossa, arXiv:1308.2962 [gr-qc].
- [11] P. Wu, H. W. Yu, Phys. Lett. **B693**, 415 (2010).
- [12] G. R. Bengochea, Phys. Lett. **B695**, 405 (2011).
- [13] L. Iorio and E. N. Saridakis, Mon. Not. Roy. Astron. Soc. **427**, 1555 (2012).

- [14] T. Wang, Phys. Rev. **D84**, 024042 (2011); R. -X. Miao, M. Li and Y. -G. Miao, JCAP **1111**, 033 (2011); C. G. Boehmer, A. Mussa and N. Tamanini, Class. Quant. Grav. **28**, 245020 (2011); M. Hamani Daouda, M. E. Rodrigues and M. J. S. Houndjo, Eur. Phys. J. C **71**, 1817 (2011); R. Ferraro, F. Fiorini, Phys. Rev. D **84**, 083518 (2011); M. H. Daouda, M. E. Rodrigues and M. J. S. Houndjo, Eur. Phys. J. C **72**, 1890 (2012); P. A. Gonzalez, E. N. Saridakis and Y. Vasquez, JHEP **1207**, 053 (2012); H. Wei, X. -J. Guo and L. -F. Wang, Phys. Lett. B **707**, 298 (2012); S. Capozziello, P. A. Gonzalez, E. N. Saridakis and Y. Vasquez, JHEP **1302** (2013) 039; K. Atazadeh and M. Mousavi, Eur. Phys. J. C **72**, 2272 (2012).
- [15] W. -S. Zhang, C. Cheng, Q. -G. Huang, M. Li, S. Li, X. -D. Li and S. Wang, Sci. China Phys. Mech. Astron. **55**, 2244 (2012).
- [16] V. F. Cardone, N. Radicella and S. Camera, Phys. Rev. D **85**, 124007 (2012).
- [17] A. A. Starobinsky, JETP Lett. **86**, 157 (2007).
- [18] S. Basilakos, S. Nesseris and L. Perivolaropoulos, Phys. Rev. D **87**, 123529 (2013).
- [19] W. Hu and I. Sawicki, Phys. Rev. D, **76**, 064004 (2007).
- [20] Weitzenböck R., *Invarianten Theorie*, Nordhoff, Groningen (1923).
- [21] R. Dave, R. R. Caldwell and P. J. Steinhardt, Phys. Rev. D, **66**, 023516 (2002).
- [22] R. Gannouji, B. Moraes and D. Polarski, JCAP, **62**, 034 (2009).
- [23] A. Lue, R. Scossimarro, and G. D. Starkman, Phys. Rev. D, **69**, 124015 (2004).
- [24] E. V. Linder, Phys. Rev. D, **72**, 043529 (2005).
- [25] F. H. Stabenau and B. Jain, Phys. Rev. D, **74**, 084007 (2006).
- [26] P. J. Uzan, Gen. Rel. Grav., **39**, 307 (2007).
- [27] S. Tsujikawa, K. Uddin and R. Tavakol, Phys. Rev. D, **77**, 043007 (2008).
- [28] P. J. E. Peebles, *Principles of Physical Cosmology*, Princeton University Press, Princeton New Jersey (1993).
- [29] V. Silveira and I. Waga, Phys. Rev. D, **50**, 4890 (1994).
- [30] L. Wang and J. P. Steinhardt, Astrophys. J, **508**, 483 (1998).
- [31] E. V. Linder, Phys. Rev. D, **70**, 023511 (2004); E. V. Linder, and R. N. Cahn, Astrop. Phys., **28**, 481 (2007).
- [32] S. Nesseris and L. Perivolaropoulos, Phys. Rev. D **77**, 023504 (2008).
- [33] G. Dvali, G. Gabadadze, M. Porrati, Phys. Lett. B **485**, 208 (2000).
- [34] Y. Gong, Phys. Rev. D, **78** 123010 (2008).
- [35] H. Wei, Phys. Lett. B., **664**, 1 (2008).
- [36] Y.G. Gong, Phys. Rev. D, **78**, 123010 (2008) X.-y Fu, P.-x Wu and H.-w, Phys. Lett. B., **677**, 12 (2009).
- [37] S. Tsujikawa, R. Gannouji, B. Moraes and D. Polarski, Phys. Rev. D, **80**, 084044 (2009).
- [38] S. Basilakos and P. Stavrinou, Phys. Rev. D, **87**, 043506 (2013).
- [39] T. D. Saini, S. Raychaudhury, V. Sahni, and A. A. Starobinsky, Phys. Rev. Lett., **85**, 1162, (2000); D. Huterer, and M. S. Turner, Phys. Rev. D, **64**, 123527 (2001).
- [40] D. Polarski and R. Gannouji, Phys. Lett. B **660**, 439 (2008).
- [41] A. B. Belloso, J. Garcia-Bellido and D. Sapone, JCAP, **1110**, 010 (2011).
- [42] C. Di Porto, L. Amendola and E. Branchini, Mon. Not. Roy. Astron. Soc. **419**, 985 (2012).
- [43] M. Ishak and J. Dosset, Phys. Rev. D, **80**, 043004 (2009).
- [44] R. Zheng, Q. -G. Huang, JCAP **1103**, 002 (2011).
- [45] R. Myrzakulov, Entropy, **14**, 1627 (2012), arXiv:1212.2155
- [46] R. Ferraro, AIP Conf. Proc. **1471**, 103 (2012), arXiv:1204.6273
- [47] S. H. Chen, J. B. Dent, S. Dutta and E. N. Saridakis, Phys. Rev. D **83**, 023508 (2011); J. B. Dent, S. Dutta, E. N. Saridakis, JCAP **1101**, 009 (2011). K. Izumi and Y. C. Ong, JCAP **1306**, 029 (2013).
- [48] E. V. Linder, Phys. Rev. D, **80**, 123528, (2009).
- [49] Bamba, K., Geng Chao-Qiang, Lee Chung-Chi, Luo Ling-Wei, JCAP **1101**, 021 (2011).
- [50] W. Fang, S. Wang, W. Hu, Z. Haiman, L. Hui and M. May, Phys. Rev. D **78**, 103509 (2008).
- [51] P. Wu and H. W. Yu, Eur. Phys. J. C **71**, 1552 (2011).
- [52] H. Akaike, IEEE Transactions of Automatic Control, **19**, 716 (1974); N. Sugiura, Communications in Statistics A, Theory and Methods, **7**, 13 (1978).
- [53] N. Suzuki, D. Rubin, C. Lidman, G. Aldering, R. Amanullah, K. Barbary, L. F. Barrientos and J. Botyanszki *et al.*, Astrophys. J **746**, 85 (2012).
- [54] C. Blake, E. Kazin, F. Beutler, T. Davis, D. Parkinson, S. Brough, M. Colless and C. Contreras *et al.*, Mon. Not. Roy. Astron. Soc. **418**, 1707 (2011).
- [55] W. J. Percival, Mon. Not. Roy. Astron. Soc., **401** 2148 (2010).
- [56] G. Hinshaw *et al.* [WMAP Collaboration], Astrophys. J. Suppl. **208**, 19 (2013) [arXiv:1212.5226 [astro-ph.CO]].
- [57] L. Samushia, W. J. Percival and A. Raccanelli, Mon. Not. Roy. Astron. Soc. **420**, 2102 (2012).
- [58] S. Basilakos, Int. J. Mod. Phys. D **21**, 1250064 (2012).
- [59] S. Basilakos and A. Pouri, Mon. Not. Roy. Astron. Soc., **423**, 3761 (2012).
- [60] M. J. Hudson and S. J. Turnbull, Astrophys. J. Let. **751**, 30 (2012).
- [61] L. Samushia, B. A. Reid, M. White, W. J. Percival, A. J. Cuesta, L. Lombriser, M. Manera and R. C. Nichol *et al.*, Mon. Not. Roy. Astron. Soc. **429**, 1514 (2013).
- [62] C. Di Porto and L. Amendola, Phys. Rev. D, **77**, 083508 (2008).
- [63] J. Dossett, M. Ishak, J. Moldenhauer, Y. Gong and A. Wang, JCAP **1004**, 022 (2010).
- [64] B. Li, T. P. Sotiriou and J. D. Barrow, Phys. Rev. D **83**, 064035 (2011);
- [65] C. M. Will, Living Rev. Rel. **9**, 3 (2006); Q. G. Bailey, R. D. Everett and J. M. Overduin, Phys. Rev. D **88**, 102001 (2013);